Wegener Center
SCIENTIFIC REPORT
102 | 2024

Double jet stream states and impacts on European heatwaves with a special focus on Austria

Martin Kriegl

February 2024

Climate Change Graz
Field of Excellence
University of Graz

Wegener Center

UNI GRAZ

The Wegener Center for Climate and Global Change is an interdisciplinary, internationally recognized research and graduate education institute of the University of Graz that is pooling the University's expertise in Climate, Environmental and Global Change. It brings together research teams and scientists from fields such as geophysics and climate physics, meteorology, economics, geography, and social sciences. At the same time, close links are maintained and further developed with many national and international cooperation partners. The research interests range from monitoring, analysis, and modeling of climate and environmental change to the investigation of climate change impacts and the analysis of the human dimensions of these changes related to mitigation, adaptation, and loss & damage. More information at **www.wegcenter.at**.



Alfred Wegener (1880 – 1930), after whom the Wegener Center is named, was founding holder of the University of Graz Geophysics Chair (1924 – 1930). In his work in the fields of geophysics, meteorology, and climatology he was a brilliant scientist and scholar, thinking and acting in an interdisciplinary way, far ahead of his time with this style. The way of his ground-breaking research on continental drift is a shining role model. His sketch on the relations of continents based on traces of an ice age about 300 million years ago (left) as basis for the Wegener Center Logo is thus a continuous encouragement to explore equally innovative ways: paths emerge in that we walk them (motto of the Wegener Center).

This report is the result of a master thesis work completed in December 2023.

SR 102 | 2024 Double jet stream states and impacts on European heatwaves with a special focus on Austria

ISBN 978-3-9505053-1-3 February 2024

Suggested citation:
Kriegl, M. (2024), Double jet stream states and impacts on European heatwaves with a special focus on Austria, Wegener Center Scientific Report 102-2024, Wegener Center Verlag, University of Graz, Austria, February 2024. ISBN 978-3-9505053-1-3
(c) 2023 Wegener Center Verlag, University of Graz, Austria

The usage of images, tables, or texts of this Scientific Report is permitted for non-commercial purposes if appropriate credit is given.
For any other purposes, please contact: wegcenter@uni-graz.at



Publishing institution:
Wegener Center for Climate and Global Change, University of Graz
Brandhofgasse 5, 8010 Graz, www.wegcenter.at

Contact: Martin Kriegl
martinkriegl@outlook.com

Martin Kriegl, BSc

Double jet stream states and impacts on European heatwaves with a special focus on Austria

Master's Thesis
to achieve the university degree of
Master of Science

Master's degree programme:
Environmental System Sciences / Climate Change and Environmental Technology

submitted to

Graz University of Technology

Supervisor
Univ.-Prof. Mag. Dr. Andrea K. Steiner

Wegener Center for Climate and Global Change
University of Graz, Austria

Graz, December 2023

Abstract

Double jet stream states are a special configuration of the jet stream in which the jet stream splits into two distinct branches. Persistent weather conditions can prevail in the centre, which is particularly important for prolonged weather extremes. This thesis investigates trends in the occurrence and frequency of double jet stream configurations and their relationship to heatwaves in Europe with a special focus on Austria. Two algorithms are developed for the detection of double jets and heatwaves. They are applied to ERA5 reanalysis data for the extended summer period (May to October) from 1979 to 2022. The results show that, on average, a double jet event was present over the European area on 30 percent of all days in the period studied. No significant increase or decrease was found for the frequency of double jet events over time. The number of heatwave days in Europe, however, has doubled since 1979, and even a tripled for the Western and Eastern European subregions. Findings show that a double jet event is particularly relevant for heatwave occurrences in Europe north of 50°N. Here, 30 percent to a maximum of 60 percent of all heatwaves can be attributed to a double jet event. A significant link between double jets and heatwaves can be established for the subregions of Western Europe, Eastern Europe, and Northern Europe. The strongest influence is found in Northern Europe, where a statistically significant correlation between heatwave days and double jet days per year was established (correlation coefficient = 0.47, p-value = 0.01). Furthermore, longer double jet events can be connected with more intense heatwaves in Northern Europe. For the region of Austria, no statistically significant connection between double jets and heatwaves was detected. The results obtained in this thesis help to understand the characteristics and the effects of double jet stream states in recent years. They show that double jets have an important influence on the occurrence of heatwaves, especially in the northern parts of Europe.

Kurzfassung

Doppeljetstreams sind eine besondere Konfiguration des Jetstream, bei der sich der Jet in zwei Zweige aufspaltet. In der Mitte können anhaltende Wetterbedingungen herrschen, was besonders wichtig für lang anhaltende Wetterextreme ist. In dieser Arbeit werden Trends im Auftreten und in der Häufigkeit von Doppeljetstream-Konfigurationen und ihre Beziehung zu Hitzewellen in Europa mit einem speziellen Fokus auf Österreich untersucht. Es werden zwei Algorithmen für die Detektion von Doppeljets und Hitzewellen entwickelt. Diese werden auf ERA5-Reanalysedaten für den erweiterten Sommer (Mai bis Oktober) von 1979 bis 2022 angewandt. Die Ergebnisse zeigen, dass im Durchschnitt an 30 Prozent aller Tage im untersuchten Zeitraum ein Doppeljet-Event über dem europäischen Gebiet auftrat. Es wurde keine signifikante Zunahme oder Abnahme der Häufigkeit von Doublejet-Events im Laufe der Zeit festgestellt. Die Zahl der Hitzewellentage in Europa hat sich jedoch seit 1979 verdoppelt und in West- und Osteuropa sogar verdreifacht. Die Ergebnisse zeigen, dass ein Doublejet-Event besonders relevant für Hitzewellen in Europa nördlich von 50°N ist. Hier können 30 Prozent bis maximal 60 Prozent aller Hitzewellen mit einem Doublejet-Event in Verbindung gebracht werden. Ein signifikanter Zusammenhang zwischen Doppeljets und Hitzewellen kann für die Teilregionen Westeuropa, Osteuropa und Nordeuropa festgestellt werden. Der stärkste Einfluss ist in Nordeuropa feststellbar, wo eine statistisch signifikante Korrelation zwischen Hitzewellentagen und Doppeljet-Tagen pro Jahr festgestellt wurde (Korrelationskoeffizient = 0.47, p-Wert = 0.01). Außerdem können längere Doppeljet-Events mit intensiveren Hitzewellen in Nordeuropa in Verbindung gebracht werden. Für die Region Österreich lässt sich kein statistisch signifikanter Zusammenhang zwischen Doppeljets und Hitzewellen feststellen. Die in dieser Arbeit gewonnenen Ergebnisse tragen dazu bei, die Charakteristika und die Auswirkungen von Doublejetstream-Konfigurationen in den letzten Jahren zu verstehen. Sie zeigen, dass Doppeljets einen wichtigen Einfluss auf das Auftreten von Hitzewellen haben, insbesondere in den nördlichen Teilen Europas.

Acknowledgments

First and foremost, I would like to thank my supervisor Univ.-Prof. Mag. Dr. Andrea Steiner for her guidance and support. I would also like to say a big thank you to Moritz Pichler, MSc. for his time and good advice, which often helped me out when I came to a dead end. Furthermore I want to thank everybody at Wegener Center who supported me during the work on this thesis.

A special thanks goes to all my friends and study colleagues who have stood by my side throughout my academic journey.

Finally I would also like to thank the "Gemeinnützige Privatstiftung zur Förderung der Forschung auf dem Gebiet der Versicherungswirtschaft", which supported this work with a grant.

Contents

1. Introduction **1**

2. Theoretical Background **3**
2.1. Climate Dynamics 3
2.2. The Jet Stream and Weather 7
2.3. Changes with Climate Change 9
2.4. Observed Changes and Current Research 11

3. Data and Methods **15**
3.1. Data 15
3.2. Methods 18
3.2.1. Double Jet Stream Detection 18
3.2.2. Heatwave Detection 19
3.2.3. Statistics 20
3.2.4. Links of Double Jet Stream States and Heatwaves . . . 20

4. Results **25**
4.1. Double Jet Stream Variability 25
4.1.1. Double Jet Stream Occurrence and Frequency 25
4.1.2. Longest Double Jet Stream Events 26
4.2. Extended Summer Heatwaves 29
4.2.1. Europe 29
4.2.2. Western Europe 29
4.2.3. Eastern Europe 30
4.2.4. Northern Europe 31
4.2.5. Austria 31
4.3. Connection of Double Jet Events and Heatwaves 36
4.3.1. Results Monte-Carlo Analysis 36
4.3.2. Linear Correlation between Double Jets and Heatwaves 40
4.3.3. Spatial Impact of the Double Jet Stream on Heatwaves in Europe 43
4.3.4. Persistent Double Jet Events and Severe Heatwaves . . 44

5. Discussion **51**
5.1. Double Jet Stream Frequency 51
5.2. Altitude and Latitude of the Double Jet Stream 51
5.3. Variability of the Longest Double Jet Event per Year 52

5.4. Spatial Impact of the Double Jet Stream on Heatwaves in Austria 53

6. Summary and Conclusions **55**

A. Latitude and Altitude of the Double Jet Stream over Time **61**

B. Double Jet Events with a certain Event Duration over Time **63**

List of Figures **65**

List of Tables **67**

Bibliography **71**

1. Introduction

Jet streams are strong bands of fast-flowing wind in the Earth's troposphere near the tropopause that encircle the globe. Their flow around the globe is characterised by a wave-like, meandering pattern. The strongest winds are found at an altitude of 10 to 12 km. They have a relatively narrow vertical width of often less than 5 km. (Woollings, 2019). Jet streams have a great influence on weather patterns in Europe and, therefore, also in Austria. High- and low-pressure systems move along the jet stream. Therefore, the jet stream's position, strength, and branching are crucial for surface weather. With ongoing anthropogenic climate change and resulting changes in the atmospheric circulation, the jet stream's behavior could also change, which would affect weather phenomena. One phenomenon that could occur more frequently is the double jet stream. Here, the jet splits into two narrow branches of wind, between which persistent weather conditions can prevail (Stendel et al., 2021). This is often connected with the occurrence of a so-called blocking event. A blocking event describes a scenario, where a persistent stationary high pressure system blocks the westerly flow at mid-latitudes for several days to weeks, i.e. the regular propagation of the jet stream is blocked and a persistent state is induced, that preserves the current weather conditions (Brunner et al., 2017). However, until recently, no clear evidence has been found that double jet stream states already occur more frequently due to climate change (Stendel et al., 2021).

Weather extremes are another feature heavily influenced by global warming, where changes are already visible (Seneviratne et al., 2021). Especially in Europe, heatwaves have become more frequent and more persistent in recent years (Rousi et al., 2022a). Heatwaves can have severe influences on human societies, from an increase in heat-related deaths, severe heat stress in cities, water scarcity in certain regions, to crop failures. Connected with that is a decline in global food production, leading to lower food security (Bednar-Friedl et al., 2022; Kornhuber et al., 2020; Messori et al., 2022). Drivers of heatwaves can be diverse, from ocean circulations and atmospheric phenomena, to regional geographic features (Perkins, 2015). The jet stream and associated double jet stream states are also assumed to play a role in the occurrence of heatwaves (Mann et al., 2017). However, there is no clear evidence, and it is still an open question, if an effect of double jet stream configurations on the more frequent occurrence and persistence of heatwaves can already be observed (Stendel et al., 2021).

This thesis contributes to answering the following questions: Is a trend in the occurrence of double jet stream states over Europe over the last decades detectable? What are the trends in the occurrence of heatwaves in Europe? Is there a detectable influence of double jet streams on the occurrence of heatwaves in Europe and particularly in Austria?

By analysing fifth generation European Centre for Medium-Range Weather Forecasts atmospheric reanalysis data (ERA5 reanalysis data), double jet stream configurations over Europe are detected and the results are examined to determine double jet characteristics and whether these configurations show a recent trend. Heatwaves are detected for different European regions, and in particular for Austria. These heatwaves are analysed together with the identified double jet stream events. It was determined if there is a significant relationship between them, and if there is a recent trend in the potential relationship. Connecting double jet stream events over Europe in summer to European heatwaves could provide some insights into how the jet stream has behaved in recent decades, how the jet stream might evolve in the future, and what this might mean for heat extremes.

Chapter 2 provides an overview of fundamental processes for the genesis of the jet stream and its properties and characteristics. Also, the impact of the jet stream on weather and weather extremes is discussed, as well as changes with climate change and ongoing research based on climate models and observations. The data used, and the methodology for developing the detection algorithm for double jet stream states and heatwaves are described in Chapter 3, along with the methods used to investigate if there is a statistically significant connection between them. The results of the analysis are presented in Chapter 4, followed by a discussion in Chapter 5. A summary and conclusions are given in Chapter 6.

2. Theoretical Background

The climate system can be roughly categorized into five main components: The atmosphere, the hydrosphere, the cryosphere, the land surface, and the biosphere. The characteristics and dynamics of the climate system are made up by the behavior of these components and the interactions between them. The jet streams are part of the atmosphere and crucial for the atmospheric circulation. The atmosphere is the gaseous shell that encompasses the Earth. It is also the most rapidly changing element of the climate system (Baede et al., 2001).

Therefore, a fundamental understanding of the climate system and its mechanisms is necessary to understand the occurrence and significance of jet streams.

2.1. Climate Dynamics

The Sun is the ultimate driver of all climatic processes on Earth and, therefore, also the driver of all atmospheric dynamics. Due to the approximately spherical structure of Earth, insolation is higher at the equator than at the poles. This is called "differential heating". This insolation difference leads to a global balancing motion of energy, which manifests through phenomena such as ocean currents or the circulation of air masses. Through such phenomena, the energy surplus at low latitudes is transported to higher latitudes. Within the atmosphere, this energy transport involves the movement of warm air masses towards the poles and the movement of cold air masses towards the equator. This transport would form a single large convection cell on a stationary earth. However, such a cell is unstable due to Earth's rotation and the resulting forces. In reality, the circulation occurs in three distinct cells; the Hadley cell, the Ferrell cell, and the Polar cell (MetOffice, 2018; Stendel et al., 2021).

As can be seen in Figure 2.1, among the three circulation cells, the Hadley cell is the one that is nearest to the equator. The air warms due to insolation; therefore, the air expands and rises. Rising air cools down, which leads to rainfall and clouds. Low-pressure systems are formed that are known as the Intertropical Convergence Zone. The air continues to rise until it reaches the top of the troposphere, near the tropopause, located at approximately 18 kilometers altitude in the tropics. Afterwards, the air spreads out north- and

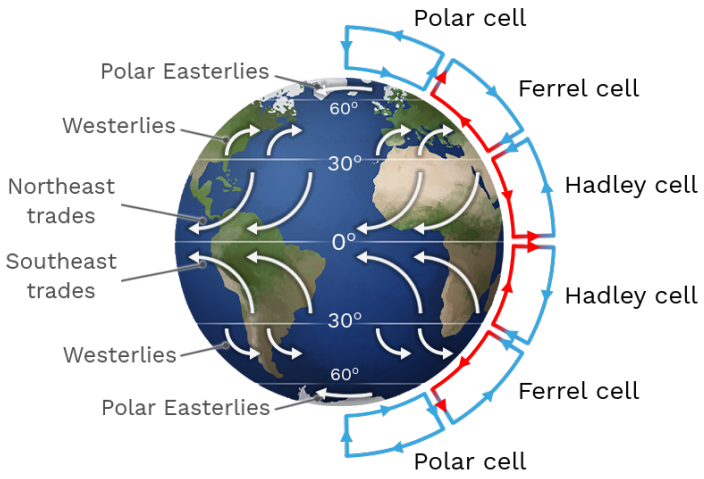


Figure 2.1.: The three large circulation cells and their approximate position above Earth, adapted from *Leyva (2018)*

southward, once more cooling down and becoming denser. At around 30° latitude North and South, the air sinks back towards Earth's surface, which leads to high-pressure systems. From here, the air moves to the equator through the trade winds, closing the Hadley cell.

The same thing occurs at around 60° latitude. Warmer air rises, which leads to clouds and rain, thus forming a low-pressure system, the subpolar low. The air flows toward the poles, where it gets colder and denser, and sinks. The underlying air is displaced by the sinking air, and it flows in the direction of lower latitudes, to around 60° latitude, forming the Polar circulation cell.

In between those two cells, there is now one cell left. The Hadley cells are driven by the temperature gradient between the equator and the mid-latitudes, and the Polar cells by the temperature gradient between the mid-latitudes and the poles. In both cells, air rises in the warmer regions and flows poleward; therefore, the convection cells are called thermally direct. The Ferrel cell, however, is thermally indirect; it has a different flow direction than the other cells. Warm air rises at around 60° latitude and flows towards the equator where it sinks together with the Hadley cell. At the surface, the air flows back towards the poles which leads to the formation of Westerlies, persistent winds that flow from west to east, in contrast to the trade winds, which flow from east to west.

The jet streams occur at the borders between these different cells, as can be observed in Figure 2.2. The polar jet is located at the boundary between Polar and Ferrel cell, the subtropical jet is located at the boundary between Ferrel and Hadley cell. These strong wind currents arise because of the large circulation cells. The temperature gradient that leads to rising or sinking

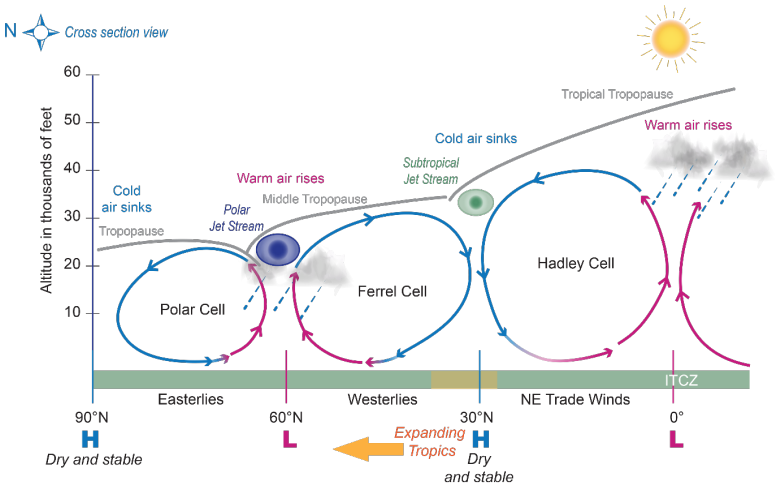


Figure 2.2.: Vertical view of the idealized atmospheric circulation, adapted from *Perlwitz et al. (2017)*

air forms high- and low-pressure areas. Since the wind speed at that height is generally high, the air flows fast from high-pressure to low-pressure areas. Nevertheless, this does not happen in a straight line; the Coriolis effect shows its impact here, and the wind gets deflected. This deflection is primarily governed by the conservation of angular momentum due to Earth's rotation.

$$\vec{F}_C = m \cdot \vec{a}_C = -2 \cdot m \cdot \vec{\omega} \times \vec{v}' \tag{2.1}$$

In Equation 2.1, the Coriolis force ($\vec{F_C}$) is expressed as the product of the mass of the moving air mass (m) and the acceleration ($\vec{a_C}$), where the acceleration is further defined as -2 * $\vec{w}$ x $\vec{v}$. Here, $\vec{w}$ represents the angular velocity of the Earth, and $\vec{v}$ represents the velocity of the moving air mass in a rotating reference frame. The Coriolis force is directly proportional to the speed of the moving air mass. Therefore, when the wind blows at high speeds, the Coriolis effect becomes more pronounced. Consequently, air that moves poleward is deflected eastward, resulting in the formation of the so called Westerlies (Goosse, 2015). The narrow width of the jet stream emerges from the large temperature difference at the boundaries. That temperature difference leads to a strong pressure gradient, which leads to concentrated wind currents. Together with the Coriolis effect the strong westerly air current occurs. However, even though the subtropical and the polar jet can be pictured as separate wind bands, this is in reality often not the case. The extent of the jet stream varies over time; often, the two jets are merged into one single band, but one jet can also split into two branches (Stendel et al., 2021).

Another striking property of jet streams is the meandering structure, the

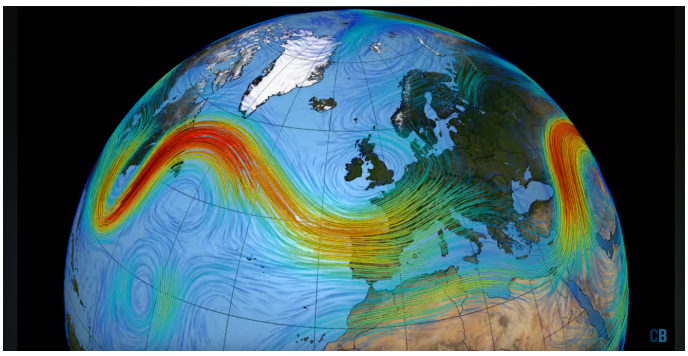


Figure 2.3.: The subpolar jet stream over Europe and the Atlantic with the characteristic meandering pattern. The colored streamlines illustrate the wind speed, dark red indicate the fastest wind speeds. Figure adapted from *NASA/Goddard Space Flight Center Scientific Visualization Studio (2011)*.

wavelike patterns around the globe, as can be seen in Figure 2.3. These patterns occur due to several reasons. Interactions with Earth's surface, mountain ranges, oceanic temperatures, or other large influences shape the flow pattern of the jet. Another essential reason is the conservation of vorticity. That means if a parcel of air moves towards the poles, the planetary vorticity of the parcel increases because the vertical axis aligns more closely with the Earth's axis. To compensate for that, the relative vorticity must decrease, meaning that the parcel must spin opposite to the Earth. That leads to a wavelike pattern. The theory of such flow patterns due to Earth's rotation was first described by Carl-Gustaf Rossby, a Swedish meteorologist (Woollings, 2019). Therefore, such Coriolis-balanced large planetary waves in the atmosphere, like the waves we can observe in the jet stream flow, are called Rossby waves. Besides atmospheric Rossby waves, there are also oceanic Rossby waves. But in the context of this thesis, "Rossby waves" always refer to the wave patterns associated with the jet stream. Due to the decrease in relative vorticity, Rossby waves would propagate to the west. However, the westerly winds deflect the waves towards the east. These two processes can also balance each other, and the propagating wave becomes a stationary wave. The Rossby wave is then fixed in space and forms a persistent pattern. However, they are not stationary forever. Usually these stationary waves exist for a few days up to weeks. Therefore, such a state is called quasi-stationary. This is important in order to distinguish such shorter-term patterns from stationary waves that result out of a multiple-year seasonal average, where normally land-sea contrasts or mountain ranges are responsible for the wave pattern (Goosse, 2015; Nugent and DeCou, 2019; Stendel et al., 2021).

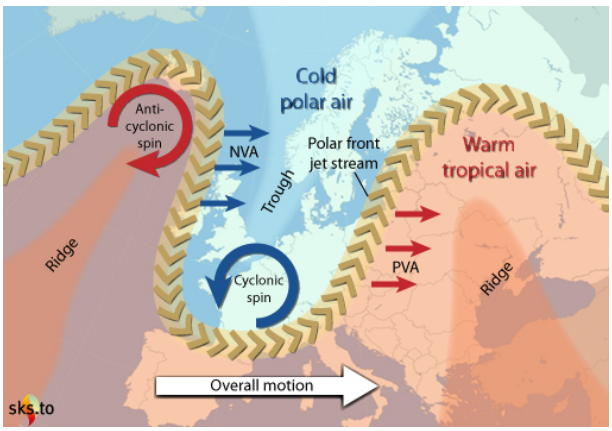


Figure 2.4.: The jet stream over Europe and the influence on weather. Negative Vorticity Advection (NVA) occurs ahead of ridges as air with clockwise rotation is transported eastward, causing air to sink and contributing to stable weather conditions and the development of high-pressure systems. Positive Vorticity Advection (PVA) occurs ahead of troughs as air with counterclockwise rotation is advected eastward, causing air to rise and contributing to unsettled weather and the development of low-pressure systems. Figure adapted from *Garrett (2013)*

.

2.2. The Jet Stream and Weather

The polar jet stream in the Northern hemisphere plays a crucial role in European weather. On the polar side of the Rossby waves, cold low-pressure troughs are formed and on the mid-latitude side warm high-pressure ridges. These weather patterns are moving along with the jet stream. Depending on where the ridges and troughs are located over Europe, the skies are either blue and sunny or rainy and cold, see Figure 2.4. Therefore, the jet stream's position is used in weather forecasting and can be seen in many weather maps. Jet streams influence the weather to a large extent. Often, weather extremes such as flooding, heatwaves, or cold spells can be attributed to the jet stream. During such extreme weather events, the jet stream is often wavier, which means that more high-amplitude Rossby waves are present (Coumou et al., 2014). A higher amplitude means that the jet extends farther into the colder polar and the warmer tropical regions, respectively. Cold or warm air travels along the jet, which results in an enhanced temperature gradient along the waves. In combination with quasi-stationary waves, this can lead to long-lasting weather extremes. Due to large ridges and throughs, contrasting weather extremes may occur on both sides of the jet stream. (Xu et al., 2022).

Atmospheric blocking is another weather phenomenon linked to the jet stream that can lead to persistent weather patterns and extreme events. Blocking may occur when a high-pressure system, known as an anticyclone,

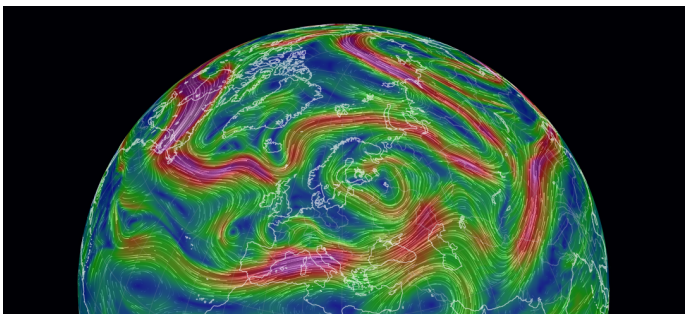


Figure 2.5.: A double jet stream structure over Europe. There are two branches of fast flowing wind and in between a center with a return flow above Scandinavia and north-eastern Europe. The colours illustrate the wind speed with purple as the fastest wind speeds. Figure adapted from *Beccario (2023)*.

forms at a ridge in the jet stream. It is called "anticyclone" because of the clockwise rotation of air around the high-pressure region, as opposed to a "cyclone", which is a low-pressure system where winds blow counterclockwise around the low-pressure center; in the Southern Hemisphere this is reversed. Such an anticyclone can hinder the atmospheric wave propagation across the hemisphere. As a result, the jet stream flows around this anticyclone, causing large-scale waves to develop in the atmosphere. These persistent waves contribute to prolonged weather conditions associated with atmospheric blocking, such as heatwaves, cold spells, or heavy rainfall (Lupo, 2021).

Depending on the season, the influence of the jet stream can be different. In winter, the jet is generally stronger and less wavy due to the enhanced temperature gradient between the poles and the tropics. However, this vortex can sometimes break; the jet shifts away or breaks into sub-jets. In that case, Arctic air can reach further southward, leading to long-lasting cold spells. In summer, the jets are weaker and shift towards the pole. Under so-called quasi-resonant conditions heatwaves and droughts may occur all over the Northern Hemisphere. Quasi-resonant conditions mean the occurrence of persistent high-amplitude quasi-stationary Rossby waves. Possible drivers of quasi-resonant conditions could be a weakening of the jet flow or an intensification of Rossby wave interaction, where two or more waves amplify or reinforce each other (Coumou et al., 2014; Stendel et al., 2021).

A so-called double jet stream structure can induce Rossby wave breaking and blocking events, which are highly relevant for the genesis of persistent weather patterns and weather extremes. The term "double jet stream" describes a state of the jet stream where the flow occurs not in a single band but in two distinct bands, effectively entrapping weather conditions between them, see Figure 2.5. In between the two strong wind bands, conditions are favorable for blocking events to occur. However, blocking events can also trigger the breaking of Rossby waves and subsequent double jet flow as air

must flow around the blocking anticyclone. But regardless of the order of emergence, the existence of a double jet can affect Rossby waves and foster the stagnation of ridges and troughs. Investigating and analyzing double jets could provide valuable insights into the occurrence of prolonged weather extremes and the connection to such jet stream states (Coumou et al., 2017; Rousi et al., 2022a).

Literature on double jets and the association with extreme weather events is relatively scarce. Nevertheless, some studies have demonstrated a strong correlation between double jet events and extreme weather events, even though there are uncertainties due to the high seasonal variability (Jain and Flannigan, 2021; Rousi et al., 2022a). Consequently, analyzing double jet occurrences can yield new perspectives and enhance the understanding of both the jet stream's behavior and the occurrence of linked extreme weather events in the Northern Hemisphere. Such an understanding is particular relevant in light of changing conditions resulting from climate change, which will be further explored in the subsequent chapter.

2.3. Changes with Climate Change

Ongoing climate change will likely change the jet stream's behavior. Nevertheless, what that change will look like is not so easy to determine. Two major competing drivers are the so-called polar amplification and tropical upper tropospheric warming. Since they both have different counteracting influences on the jet stream, this is called a "tug-of-war" on the jet stream (Barnes and Screen, 2015; Perlwitz, 2011).

Polar amplification describes the faster warming of polar regions in comparison to other regions of the world. To distinguish the poles it is also called Arctic amplification for the north polar region and Antarctic amplification for the south polar region. There are multiple mechanisms and feedbacks that drive this stronger warming process, like the ice-albedo and snow-albedo feedback. That means, that the reduced snow or ice cover due to global warming reduces Earth's albedo (reflectivity). Consequently, more incoming solar radiation is absorbed, and less is reflected, which leads to further warming. Therefore, such a feedback is called amplifying feedback. Since ice and snow are white, they have an especially high albedo; fresh snow has a value of 0.8 to 0.9, old snow from 0.45 to 0.9. Sea ice has an albedo value of 0.3 to 0.6. The ocean, on the other hand, has an especially low albedo from 0.05 to 0.15, making the reduction of sea ice particularly relevant. There are also other feedbacks, like interactions between cloud cover in different altitudes and insolation, that are relevant for Polar amplification as well as other remote forcing mechanisms like atmospheric heat or moisture transport into polar regions (Cohen et al., 2020; Francis and

Skific, 2015; Goosse, 2015; Stendel et al., 2021; Wu et al., 2023). Another key reason that leads to an enhanced warming of polar regions is the almost non-existing convection at high latitudes. The low angle of arriving sunlight causes that the energy flux per unit area into the surface is lower. Therefore, the air near the surface is also only slightly warmed by the surface; the stratification of the atmosphere remains stable and very little convection occurs. The atmosphere is warmed mainly by incoming warm, moist air from the tropics. Increased greenhouse gas concentration heats the near-surface atmosphere stronger. The lack of vertical mixing, due to very little convection, leads to strong surface warming (Taylor et al., 2022).

Due to the stronger warming at the poles, the overall Equator-to-Pole surface temperature gradient will be reduced. For the jet stream, which is driven by this temperature gradient, this may imply a reduction in wind speed. That reduction could result in wavier jet stream states and an enhanced meandering pattern (Alizadeh and Lin, 2021; Moon et al., 2022). This is comparable to water flowing in a strong flow over open land. If the current gets weaker, it will become unable to maintain a straight flow line and will be more easily deflected by obstacles. Such a wavier jet stream pattern can subsequently lead to quasi-resonant conditions and, therefore, to persistent extreme weather events in the Northern Hemisphere. Furthermore, the reduced temperature gradient would shift the jet stream more equatorward (Coumou et al., 2017).

In general, Arctic amplification has a greater effect in winter, as sea ice melt is greatest here. This sounds contradictory at first, but this is due to the large heat capacity of water. In summer, heat from the sun is absorbed by the ocean. In winter, the atmosphere is colder than the ocean below and the heat is released, causing sea ice to melt (Taylor et al., 2022).

While Arctic amplification is most pronounced near to the surface, tropical warming leads to higher temperatures in the upper tropical troposphere. This notable additional warming can be attributed to a reduced moist adiabatic lapse rate (Stendel et al., 2021). The moist adiabatic lapse rate characterises how the temperature of an air parcel containing water vapor decreases with height without heat exchange with the surroundings. With enhanced global warming, additional water vapor and latent heat are released into the atmosphere. As a consequence, the moist adiabatic lapse rate is reduced, i.e. the temperature decrease of an air parcel with height is reduced. This results in a more pronounced warming of the upper troposphere (Goosse, 2015; Stendel et al., 2021).

A more pronounced warming of the tropical upper troposphere would mean a shift of the global temperature gradient, but in the opposite direction and in another altitude (i.e. on tropopause level, not on surface level) as the shift resulting from polar amplification. Therefore, the jet stream would shift poleward. Since the temperature gradient gets stronger in that scenario, the

wind speed of the jet would also become stronger.

Determining which of these two mechanisms will overcome the other is challenging due to multiple factors, like short observational timescales and the high natural variability, which makes it difficult to distinguish the effects of the mechanisms from the forced response due to climate change (Connolly et al., 2023). Different studies show different results; there are also differences between modeling and observational studies. However, since this is a topic of active research and discussion, such discrepancies are also to be expected, especially with the different approaches and assumptions that are made in different studies. (Cohen et al., 2020; Fragkoulidis, 2022; Wu et al., 2023). Nevertheless, some observational studies and recent analyses allow assumptions on future development, as can be seen in the next chapter. It is also to be expected that in the future enhanced progress in understanding the changing jet stream through climate change will happen due to improved models and new observations.

2.4. Observed Changes and Current Research

Some studies find a poleward shift of the Northern Hemisphere jet stream in the recent decade 2012 to 2020 from observational data and climate models (Deng et al., 2022; Stendel et al., 2021). That shift would suggest that tropical upper tropospheric warming has a stronger effect. However, to date only a relatively small shift has been observed, and knowledge about the actual strength of the effect on the jet stream is limited. The poleward shift is evident across different seasons, but its significance varies depending on the analysis method. This means that some studies have found a shift to be statistically significant for certain seasons, while others have found no significance (Deng et al., 2022; Fragkoulidis, 2022; Maher et al., 2020; Pena-Ortiz et al., 2013; Woollings et al., 2023).

An increase in the waviness of the Northern Hemisphere jet stream was found, especially in summer over Eurasia (Alizadeh and Lin, 2021; Coumou et al., 2017; Moon et al., 2022; Rousi et al., 2022a). Arctic amplification is thought to be a possible driver. However, a direct attribution was not possible since natural and internal variability is a larger, overlaying driver and could not be separated from other influences. Additionally, large circulation patterns like the El Niño-Southern Oscillation or the North Atlantic Oscillation influence the position and strength of the jet stream (Trouet et al., 2018). Also the Pacific Decadal Oscillation is expected to impact jet variance on a multi-decadal scale. Due to the different mechanisms, there are a lot of regional variations in jet latitude and speed (Deng et al., 2022; Hallam et al., 2022; Rodriguez Solis et al., 2022).

Next to regional variations, there are as well seasonal variations. Arctic

amplification is strongest in boreal winter, while tropical upper tropospheric warming can have a larger influence in summer. Of course, these two effects can also influence each other and therefore they cannot be seen as two completely separate mechanisms that act independently of each other (Barnes and Screen, 2015; Stendel et al., 2021; Wu et al., 2023).

Overall, no apparent, significant trend in the flow of the Northern Hemisphere jet stream could be found until today. Possible reasons for this include the high internal variability, the influence of large-scale circulations,and the short time periods available for analysis. However, a recent study found an increase in vertical wind shear in the North Atlantic polar jet stream. That means that the increase of wind speed in the upper atmosphere is stronger than in the lower atmosphere. That rise in vertical wind shear can be attributed to tropical upper-tropospheric warming and can result in clear-air turbulence, which is relevant for commercial flights (Lee et al., 2019).

There is an undoubtedly increasing trend for weather extremes due to ongoing climate change. That is especially true for heatwaves in the Northern Hemisphere summer. Heatwaves are projected to be more frequent and more persistent in the future (Coumou et al., 2014; Deng et al., 2022; Kornhuber et al., 2020; Rousi et al., 2022b). The impact of heatwaves on humans and human societies is severe; possible consequences are briefly discussed in Chapter 1. Longer and more frequent heatwaves further exacerbate the problems and consequences that society must face (Bednar-Friedl et al., 2022).

While there is a clear increase in heatwave frequency and persistence, the influence of the jet stream in a changing climate is not so well understood. However, in both observational and modeled data, anomalous jet stream patterns tend to coincide with weather extremes. Anomalous means unusual latitudinal position, a slower jet, or persistent wave patterns present (Belmecheri et al., 2017; Coumou et al., 2017; Galfi and Messori, 2023). Among the unusual patterns is also the double jet stream. When a persistent double jet stream pattern is present, there is a higher likelihood that high-amplitude Rossby waves and a blocking anticyclone are present since they are considered a consequence or a prerequisite of double jet stream states, as mentioned above. They may also be two different manifestations of a common phenomenon. However, that creates conditions that foster the development of prolonged heatwaves. The existence of a double jet stream can therefore be an indicator for such an extended heatwave. Some studies show that double jet events coincide with wildfires resulting from droughts (Jain and Flannigan, 2021), that double jets are present when extreme heat events occur (Coumou et al., 2017), and that they can be used to explain the persistence and variability of heatwave trends over Eurasia (Deng et al., 2022; Rousi et al., 2022b; Rousi et al., 2022a).

However, the direct link between double jet stream states and heatwaves still needs to be clarified. Assessing double jet stream events over Europe in summer and connecting this analysis with heatwave events, as investigated in this thesis, could help to shed light on that potential link.

3. Data and Methods

3.1. Data

The data used here to detect double jet stream configurations and heatwaves are produced by the European Centre for Medium-Range Weather Forecasts (ECMWF). They are fifth generation ECMWF atmospheric reanalysis data (short ERA5 reanalysis data). "Reanalysis" means that observational data are combined with model data in a process called assimilation. This combination is done to account for spatial and temporal constraints imposed by observational measurements via satellites or surface monitoring stations and to ensure continuous, global climate data. The ERA5 reanalysis is the successor of the ERA5-Interim reanalysis and the fifth generation of climate and weather reanalysis. It has improved temporal and spatial resolution and benefits from research efforts on reanalysis and climate/weather models. The ERA5 reanalysis spans from 1950 to the present, with an hourly temporal resolution, a 31 km horizontal resolution, and 137 vertical pressure levels (Hersbach et al., 2020).

Reanalysis data allow the accurate analysis of the jet stream. Since the jet varies strongly in time and space, continuous, detailed data are necessary for the detection. It must be noted, however, that the data and the individual parameters are mostly generated by a model and therefore associated with fundamental uncertainties.

The data are distributed via the Copernicus Climate Change Service (C3S), which is part of the Copernicus Program of the European Union. The datasets are available for free download in their Climate Data Store (DOI: 10.24381/cds.adbb2d47).

Double Jet Stream Detection

ERA5 reanalysis eastward wind (u-wind) data from 1979 to 2022 with a resolution of 2.5° x 2.5° were used to study double jet stream states over Europe in the extended summer period from May to October (MJJASO). The months MJJASO were chosen because in the further analysis the detected double jet streams were analysed together with European summer heatwaves. The data were mapped on altitude levels rather than pressure levels in order to analyse the jet stream over an altitude range instead of on a single pressure level. The data, already mapped on altitude levels, were provided

from the Atmospheric Remote Sensing and Climate System Research Group (ARSCliSys) from the Wegener Center for Climate and Global Change Graz. They were available from 1979 onwards, which results in a time restriction compared to the ERA5 reanalysis data on pressure levels downloadable from the C3S, which are available from 1950 onwards. The spatial extent ranges from 10°W to 50°E and from 25°N to 80°N, which covers Europe, the Mediterranean, parts of North Africa, the Arabic Peninsula, and the North Atlantic. This can be seen in Figure 3.1. Daily values were calculated from 6-hourly daily data. The chosen altitude levels range from 8 to 13 km with a 100 m resolution.

Heatwave Detection

To identify heatwaves, ERA5 reanalysis data for 2-meter altitude temperature were used. The data covered the same time period as in the double jet analysis (the months MJJASO from 1979 to 2022) and had a spatial resolution of 0.25° x 0.25°.

The approximate Austrian region was set to extend from 9.5° to 17.0°E and from 46.5° to 49.0°N. The Austrian region with all grid points according to this definition can be seen in Figure 3.2.

To detect heatwaves in Europe, the same spatial extent was used as for the double jet stream detection. To determine more precisely the effects of heatwaves and double jets on different parts of Europe, the European region was further split into different areas: Western Europe, Eastern Europe, and Northern Europe. The extent of the Western European region was set according to Rousi et al. (2022a); from -9° to 14°E and from 36.5° to 55°N. For Eastern Europe the spatial extent was set to 14° to 32°E and from 36° to 55°N; for Northern Europe the spatial extent was set to 5° to 32°E and from 55° to 70°N. The regions can be seen in Figure 3.3. The boundaries are set to cover almost all of Europe in a meaningful way for the heatwave analysis, which ideally means continuous land without large bodies of water in between. Only land grid points were considered in the analysis. A land-sea mask was used to remove all sea grid points from the 2-meter altitude temperature data. This land-sea mask is also part of the ERA5 reanalysis data.

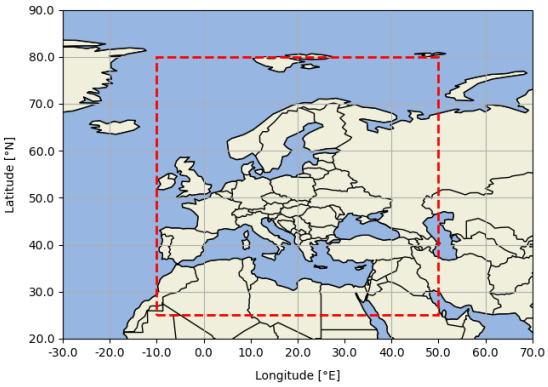


Figure 3.1.: Spatial area for the detection of double jet stream states

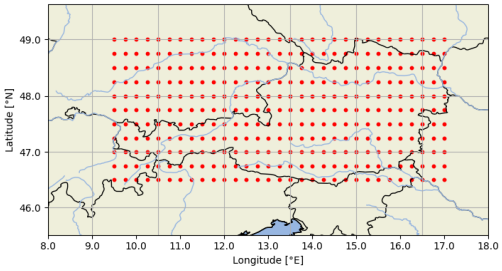


Figure 3.2.: Grid points for the analysis of Austrian heatwaves

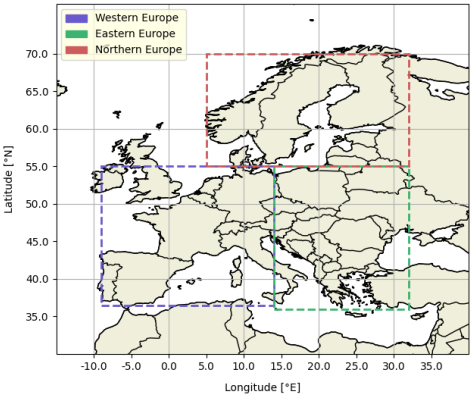


Figure 3.3.: Regions for the analysis of European heatwaves

3.2. Methods

3.2.1. Double Jet Stream Detection

There are a lot of different methods for the identification and analysis of jet streams. They differ in how they deal with the characteristics of the jet stream, i.e. the meandering, breaking, and branching, as well as the temporal resolution. An overview of different methods for the identification of jets can be found in Rikus (2018). Most of the methods make use of data on pressure levels, and more specifically the 250 hPa pressure level only. In this thesis, data for different altitude levels, as described before, are analyzed. In contrast to the use of a single pressure level, this method could gain a more precise result of the jet's position. A definition of double jet streams in the Northern Hemisphere is applied after Rousi et al. (2022a). A double jet stream must consist of the following:

- Two zonal wind maxima at approximately 40°N and 70°N
- An area of weak wind with negative wind speed anomalies between 45°N to 65°N

The wind maximum at approximately 40°N corresponds to the subtropical jet stream, and the wind maximum at approximately 70°N corresponds to the polar jet stream.

To determine the jet stream state for each day, first the longitudinal mean zonal wind for each day was calculated for the European area, which resulted in altitude-latitude planes with the longitudinal mean zonal wind for each day. A double jet stream is a large-scale pattern that must be present over the entire region to impact heatwaves in that region. The peak finding algorithm *peak local max* from the python package *scikit-image* was adapted and applied to identify the two wind maxima in the altitude-latitude planes. The threshold wind speed was set to 10 m/s, and the minimum distance between the peaks was set to 7°. In order to identify the minimum in between, the data were inverted, and the peak-finding algorithm was applied again. The threshold wind speed was set here to 5 m/s to account for small but not negative wind speeds, and the plane's borders were excluded to only find the minimum in the middle. All parameters were tested and fine-tuned by individual, manual analysis of many altitude-latitude planes. Any day where the average zonal wind speed exhibits 3 peaks in the altitude-latitude plane is counted as a day with a double jet stream present.

In Figure 3.4a, a clear double jet stream structure can be observed in the altitude-latitude plane. The subtropical jet with a maximum of around 45°N can be clearly distinguished from the polar jet stream with a maximum of around 75°N by the band of negative wind in the middle with a minimum of around 63°N. In Figure 3.4b, no double jet stream structure can be found.

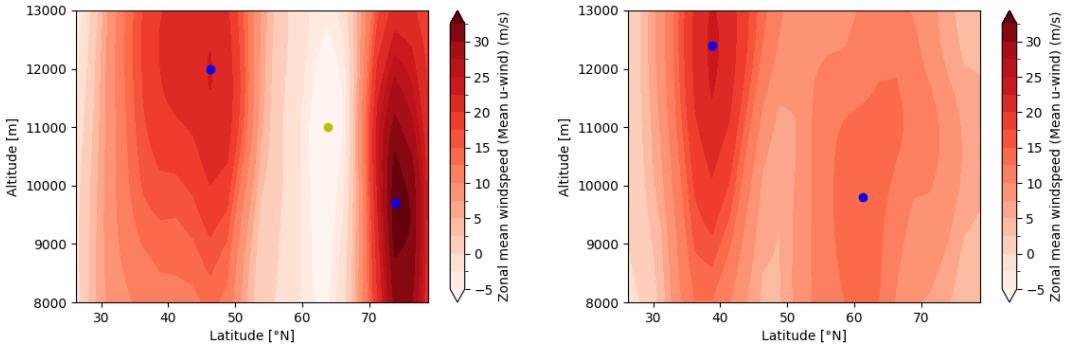


Figure 3.4.: Altitude-latitude planes for the double jet stream detection. Panel **a** shows an example of an altitude-latitude plane for a single day with a visible double jet stream after running the peak-finding algorithm. Detected positive peaks are marked by blue dots, negative peaks by green dots. In Panel **b** an example of an altitude-latitude plane with no double jet stream present can be seen. Blue dots mark the detected positive peaks; negative peaks were not found.

The jet does not split its flow into two distinct branches. Two maxima can be found; however, they are located too close to each other to form a double jet structure. The wind flow is approximately evenly distributed over the entire plane compared to a double jet stream event.

3.2.2. Heatwave Detection

There is no universal definition of a heatwave, but some essential criteria are often used in literature. Here, a definition of a heatwave was applied that was also used in a similar form by Rousi et al. (2022a), Fischer and Schär (2010), and Russo et al. (2015), among others. A grid point is defined to experience a heatwave if:

- The temperature exceeds a threshold. The daily maximum temperature has to be higher than the 90th percentile of the maximum temperature distribution of the whole period studied, based on a 15-day window.
- The temperature exceedance has a duration of at least 3 consecutive days.
- 90 percent of all grid points in a 2° x 2° window around the grid point also experience a heatwave.

Only land grid points were considered. Each grid point on a certain day has an individual threshold temperature, which is the 90th percentile of the 15-day window around that grid point on a particular day over all years in the studied period from 1979 to 2022. Whenever the daily maximum

temperature on that grid point exceeded that threshold temperature for at least 3 days in a row, the grid point experienced a heatwave. Subsequently, a rolling window was applied to all grid points individually to check for the spatial condition. When, according to the previous definition, 90 percent of the grid points within the window were experiencing a heatwave, the central grid point was considered as being in a heatwave. If such a heatwave was detected on a certain day, the day was considered as a heatwave day for the respective region.

Since Austria is relatively small, a 2°x2° window covers a very large part of the country. To determine whether there is a significant difference in the further analysis when local heatwaves are used instead of heatwaves with a large spatial extent, the heatwave analysis for Austria was carried out twice: Once according to the definition above, and once ignoring the spatial extent of the heatwave (i.e. if a single grid point experienced a heatwave, this was considered as a heatwave in Austria).

3.2.3. Statistics

A simple linear regression model (Ordinary Least Squares - short OLS) was applied to assess changes and potential trends over time in the results obtained from the double jet stream- and the heatwave detection. Simple linear regression is a statistical method used to analyze the relationship between a dependent variable and one or more independent variables (Haslwanter, 2016). In this context, time is the independent variable that is used to predict or explain changes in the dependent variables, the detected double-jet events, and the count of heatwave-days.

To compare the variance of two groups, Levene's test was applied. Two same-size groups were created from the time series of the longest double jet events per year. Levene's test assesses if the variance of these two groups is significantly different. Variance is a statistical measure that quantifies how the individual data-points spread around the mean (Haslwanter, 2016).

3.2.4. Links of Double Jet Stream States and Heatwaves

Monte-Carlo Analysis

To determine if the connection between heatwaves days and double jet stream days is statistically significant, a Monte-Carlo test was carried out. It was applied in a similar form by Brunner et al. (2017) for determining the connection of atmospheric blocking and temperature extremes.

$$HW_F^{dj} = \frac{T_{hw}^{dj}}{T^{dj}} \tag{3.1}$$

$$HW_F^{r} = \frac{T_{hw}^{r}}{T^{r}} \tag{3.2}$$

First, according to equation 3.1, the heatwave frequency $HW^{\mathrm{dj}}{}_{\mathrm{F}}$ was calculated by dividing the total number of days with both a double jet event and a heatwave present ($T^{\mathrm{dj}}{}_{\mathrm{hw}}$) by the total number of days with a double jet event present (T^{dj}). The resulting value represents the fraction of days on which a heatwave occurred when a double jet event occurred simultaneously. This was done for the different European subregions and Austria. The larger the region, the more likely it is, that spatially separate heatwaves overlap in time. This results in a very long heatwave-days timeline, that is needed in this analysis. Therefore, it was not meaningful to carry out this analysis for the whole of Europe.

To assess the statistical significance of the connection between heatwaves and double jet events, the Monte-Carlo test was performed with 5000 random samples according to equation 3.2. Random days T^{r} of the same number as the number of days with a double jet event T^{dj} were drawn from the entire period. For each random day, it was determined whether a heatwave occurred ($T^{\mathrm{r}}{}_{\mathrm{hw}}$) and the heatwave frequency $HW^{\mathrm{r}}{}_{\mathrm{F}}$ was calculated. The heatwave frequency $HW^{\mathrm{dj}}{}_{\mathrm{F}}$ was compared to the 90th percentile of the heatwave frequency calculated from the 5000 random samples to evaluate the statistical significance. Suppose the frequency of heatwaves is higher when a double jet event is present than the 90th percentile of the frequencies of heatwaves in the random samples. In that case, the connection between heatwaves and double jet events is considered to be statistically significant.

Linear Correlation between Double Jets and Heatwaves

To investigate a potential correlation between double-jet days and heatwave-days, Pearson's correlation coefficient was calculated for the distinct European subregions and Austria. This coefficient assesses the relationship between two variables by examining whether changes in one variable correspond to changes in the other. In this case, it is detected if the number of heatwave days is changing in a similar manner as the number of double jet days, or vice versa. Pearson's correlation coefficient can take any value from -1 to 1. 1 indicates a strong positive correlation, -1 indicates a strong negative correlation, and 0 indicates no correlation at all (Haslwanter, 2016). To account for potential trends, the annual occurrences of heatwave-days and double-jet stream days were detrended with a linear regression model before calculating Pearson's correlation coefficient.

Spatial Impact of the Double Jet Stream on Heatwaves in Europe
In order to identify the regions in Europe where the double jet has a particular impact, heatwaves were linked with double jet events. To attribute a heatwave to a double jet event, at least 60 percent of all heatwave days of a heatwave on a certain grid point must coincide with a simultaneous double jet event. This percentage was chosen due to the minimum duration of a heatwave being three days, meaning that with this overlap criterion a minimum of two days had to align with a double jet event. This guarantees that the overlap does not have to affect every day within a heatwave but the majority of days. It must be noted, that the threshold might be too low for exceptionally long heatwaves.

With this analysis the number of days per grid point can be found, that experience a heatwave while a double jet stream event occurs at the same time.

Persistent Double Jet Events and Severe Heatwaves
To examine a potential link between persistent double-jet events and more severe heatwaves, an analysis was conducted that follows a similar methodology as in Rousi et al. (2022a). First, the heatwave cumulative intensity was calculated for each heatwave according to equation 3.3. The heatwave cumulative intensity quantifies the total excess temperature during a heatwave.

$$heatwave\ cumulative\ intensity = \sum_{d=1} \sum_{i=1} (T_{max}^{i,d} - T_{max90th}^{i,d}) \tag{3.3}$$

To compute this additional heat, the temperature threshold $T_{\mathrm{max90th}}{}^{\mathrm{i,d}}$ (see section 3.2.2) was subtracted from the actual daily maximum temperature $T_{\mathrm{max}}{}^{\mathrm{i,d}}$ for every grid point, where a heatwave was detected. The resulting excess temperatures for all grid points i within a heatwave on a given day were then summed, yielding the total excess temperature for that specific day. The summation of these values across all days d within a heatwave provided the total excess heat for that heatwave.

To attribute a heatwave to a double jet event, again at least 60 percent of all heatwave days must coincide with a simultaneous double jet event. One additional limitation to this method are large regions, where heatwaves can occur in different areas without being connected. If these heatwaves overlap in time a heatwave event with a very long duration could be created, since the daily heatwave cumulative intensity is calculated for the entire region, regardless of whether the individual grid points are related. For such a resulting exceptionally long heatwave, the overlap threshold value might be too low and heatwaves cannot be linked to a double jet event.

To address this issue, the European region has been divided into three subregions, see Figure 3.3. However, it is still possible for long heatwaves to occur due to an overlap, even in the smaller distinct areas. To assess if

this overlap has a relevant impact, the number of heatwaves per grid point that coincide with a double jet event for the distinct regions was compared to the numbers obtained from the similar analysis for the whole European area. Since the analysis for the whole European area is done per grid point, there is no overlap limitation. If the two distribution patterns are consistent, the overlap limitation has no relevant impact.

As a result of this algorithm, composites of the length of double-jet events and the cumulative temperatures of the associated heatwaves were obtained for further analysis. Thus, a potential link between an increased heatwave cumulative intensity and persistent double jet events can be explored. Further, the specific regions within the studied areas where double jet events have an impact on heatwaves can be identified.

4. Results

4.1. Double Jet Stream Variability

4.1.1. Double Jet Stream Occurrence and Frequency

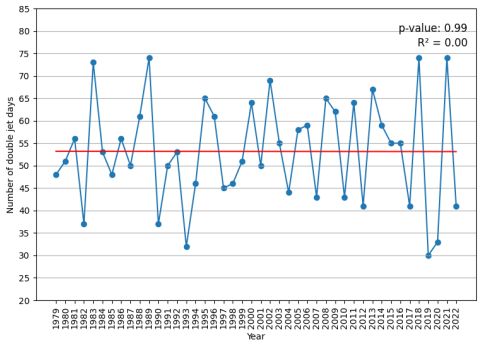


Figure 4.1.: Double jet stream days per half-year (MJJASO). The red line represents the trend as calculated with an OLS scheme. The associated p-value and the R^2-value are shown.

With a linear fit no significant trend in the number of double jet days over time in the studied period from 1979 to 2022 could be found (Figure 4.1). The number of double jet days over the studied period does not follow any observable pattern and varies greatly from year to year. In years with the fewest double jet days about 30 days are found; in years with the most double jet days, up to 75 days are found. The same is true when the number of double jet days is observed for each month of the months MJJASO individually instead of each half-year of the study period. No trend could be found, but the number of days detected varies considerably over time. Therefore, no change in the mean occurrence of double jet days can be detected from this analysis.

The frequency of double jet days per half-year can be seen in Figure 4.2a. This frequency describes the proportion of days in a half-year on which a double jet event occurred. Again, a half-year means the months MJJASO. The frequency varies considerably, which is due to the high variability of the number of double jet days in a year. Minimal frequencies are found just below 0.2, maximal frequencies at around 0.4. The mean frequency is at 0.29.

This means that, on average, a double jet event was detected on almost 30 percent of all MJJASO days in the studied period. Therefore, according to this analysis, a double jet structure is not a rare event. This frequency is general in agreement with the findings of Rousi et al., 2022a. They found a double jet frequency of 36 percent over the same time period, but only for the months of July and August and over the entire Eurasian area. They also used a different detection algorithm. All this could lead to more double jet days being detected.

The mean frequency of the jet stream occurrence over all half-years from 1979 to 2922 broken down by each month of the analysis can be seen in Figure 4.2b. The highest frequency was found in June with a double jet occurrence of about 37 percent, the lowest frequency in August with 20 percent. Thus, June is the month with the highest occurrence of double jet events across all years, followed by May (33 percent). July, September, and October have almost the same frequency (27 to 29 percent) and August is the month with the fewest double jet days.

No significant change in the mean frequency of double jet events of a certain length was found over time. Across all years, events were counted that had a minimum duration of a selected length, ranging from a duration of only one day to a duration of 12 days (see Figure B.1). Longer events did occur, but they are so rare that a frequency trend analysis with a linear regression does not provide any meaningful information. There were no significant trends for any of the event durations, the distribution over the years remained fairly constant. Therefore, an increased occurrence of longer double jet events in recent years cannot be detected by this analysis.

4.1.2. Longest Double Jet Stream Events

The longest double jet event in each year can be seen in Figure 4.3. The shortest events of those are up to 5 days, while the longest events lasted 22 days in 2013. However, that was an extraordinary long event. On average, the longest events have a duration of 11 days. No linear trend can be observed; the longest events do not become significantly longer or shorter over time.

The occurrence of the longest double jet events for each half-year broken down by each month is shown in Figure 4.4. There were a total of 43 events, one for each year from 1979 to 2022. By far the largest number of these events occurred in May, with 16 events. A large proportion of the longest events also occurred in June, with 10 events. July had only 3 of the longest events per year and August, September, and October each had 5 events.

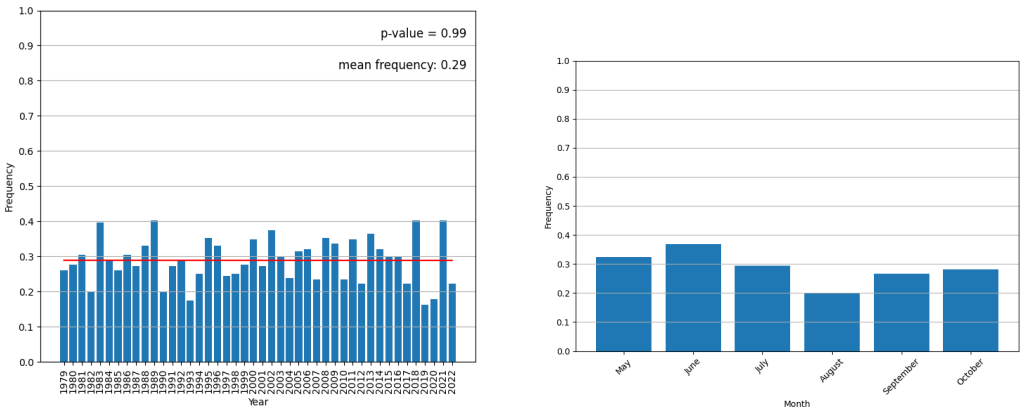
To detect a potential change in variability a Levene's test for two distinct groups was carried out. The two groups can be seen in Figure 4.3 in two distinct colors, blue and orange. However, the test did not yield a significant result; no difference between the two variances could be detected. This

suggests that there are no significant changes in the variability of the longest event durations between the two groups. Levene's test was also performed for 3 distinct groups but again no significant result was found. It was not possible to perform the test for even more groups, because with the limited number of years the sample size would be too small.

A more intriguing result can be seen in Figure 4.5. Here, the variances of the longest double jet events for each year, based on a 11-year, a 9-year and a 5-year moving window are depicted. Until about 2008, the variances are fairly consistent, ranging from around 2 to a maximum of 15. This suggests that the longest events until about 2008 had similar durations, as the values in the moving window must be similar for the resulting variance to be low and relatively consistent. However, there is a notable turning point that occurs in 2008, marked by a sudden and sharp increase in the variance value to 15 for the 11-year window variances. This value persists until 2011 and continues to rise in the following years, reaching 28 in 2015 and beyond. For the variances calculated using the 9-year window the sharp increase occurs one year later, in 2009. From here the variance also increases to a maximum value of almost 35 in 2016. The variance then decreases to a still high value of 20 in 2018. With a window size of 5, there is a sudden increase from a variance of 8 to 24 in 2011, followed by a slight decrease in the next two years and then a sharp increase again to almost 35. From here on, the variance decreases to a value of about 18 in 2020, which is still much higher than in the early years when the variance was quite stable.

This abrupt and large increase indicates that the durations of the longest jet events per year within the window are no longer similar, but vary more widely. This can also be seen in Figure 4.3. Here, the initial length of the longest event per year is quite similar in the early years. However, since the last decade, longer, but also exceptionally short event durations can be observed more often. Consequently, the behaviour of the longest event durations has evolved into a more variable pattern in recent years.

The first sharp increase in variance after the relatively even course is caused by the longest double jet event detected in the whole timeline in 2013. This is true for all three different window sizes; the increase always started when the year 2013 became part of the respective window. This unusual double jet event in 2013 was also detected by Rousi et al. (2022a), who assessed double jet states over Eurasia. It was in 3rd place for the longest events found in the period 1979 to 2022 for the months of July and August. Nevertheless, this event alone does not explain the still very high variance in the following years. The variance remains high, even though the 2013 event is no longer part of the window for all three window sizes. This underscores that also the longest events in the following years vary increasingly in length.



a) b)

Figure 4.2.: Double jet stream frequency. Panel **a** shows the double jet frequency for MJJASO from 1979 to 2022. The red line shows a OLS linear fit. The associated p-value and the mean frequency are shown. Panel **b** shows the frequency per month from 1979 to 2022.

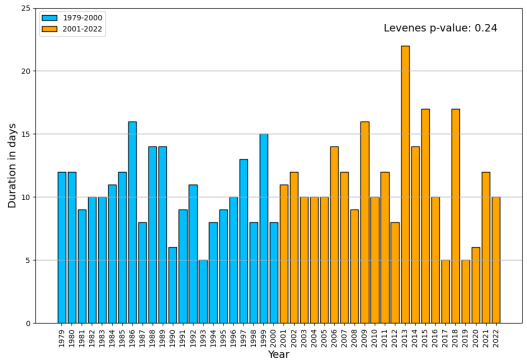


Figure 4.3.: Duration of the longest double jet event per year and comparison of the variances of the first and second half of the period with Levene's test. Both groups consisted of 21 years. The associated Levene's p-value is shown.

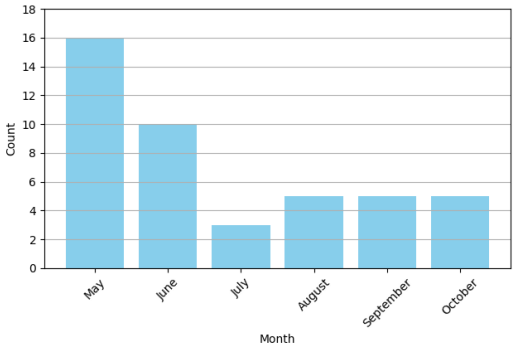


Figure 4.4.: Monthly occurrence of the longest double jet event of each half-year (see Figure 4.3). Double jet events are attributed to the month in which they begin.

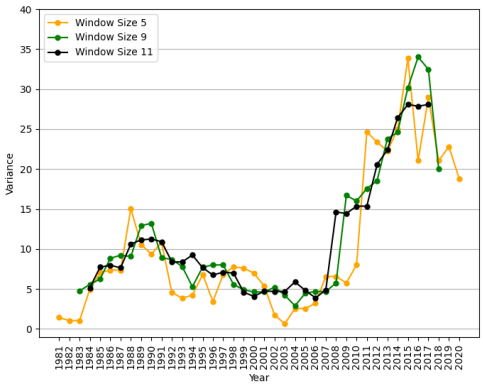


Figure 4.5.: Moving variance of the duration of the longest double jet event per year. The variances were calculated using an 11-year window (black line) to obtain the decadal variance of each year, as well as a 9-year (green line) and a 5-year window (orange line).

4.2. Extended Summer Heatwaves

4.2.1. Europe

As can be seen in Figure 4.6a the number of heatwave days per half-year in Europe has more than doubled from 1979 to 2022. More than 160 heatwave days were detected in 2022, which is almost every day in that half-year. However, these are days on which a heatwave occurred somewhere in the European area, and these heatwaves must not be spatially connected. For this reason, assessing the number of heatwave days per year for the distinct regions provides a more precise picture. Nevertheless, the overall count reveals a significant alarming increase.

Figure 4.6b shows the occurrence of heatwave days per grid point for the whole of Europe. Particularly high numbers of heatwaves over a large spatial extent are detected for the eastern part of the European area, especially Ukraine, Russia, and the Baltic countries. A more detailed analysis for the different European regions is given in the following subsections.

4.2.2. Western Europe

The number of heatwave days in Western Europe is undoubtedly increasing. Since 1979, the number of heatwave days has more than tripled, which can be seen in Figure 4.7a. This increase can be attributed to the ongoing climate change and has also been found in other studies, see Chapter 2.4.

Figure 4.7b shows the number of heatwaves on any grid point in Western Europe over all the years analysed. The highest number of heatwave occurrences is found inland where there are no large mountain ranges, especially

in France, western parts of Germany, the center of the Iberian Peninsula and in Central Britain.

At the coast, the number of heatwaves cannot be detected which is due to the land-mask and the window used for the calculation. Near the coast there is an area with a very low number of heatwaves which is due to interpolation constraints by the python-package *matplotlib*.

Over northern Italy and the western part of Austria the detected number of heatwaves per grid point is low. This may be due to the presence of the Alps, which could act as a physical barrier that hinders the expansion of heatwaves to a large spatial extent. This could also be the case for the area at the border between France and Spain, where a lower number of heatwaves were detected because the Pyrenees are located in this region.

4.2.3. Eastern Europe

In the Eastern European region, the half-yearly number of heatwave days in MJJASO has more than tripled over the observed period, as shown in Figure 4.8a. A statistically significant increase from 22 heatwave days per half-year in 1979 to 79 heatwave days per half-year in 2022 is found.

Figure 4.8b shows where the heatwaves occurred in Eastern Europe. As in Western Europe, heatwaves near the coast cannot be detected. Partly, this is due to interpolation artefacts. But also the heatwave detection algorithm used plays an important role here, as some coastal regions are simply too small to be covered by a 2°x2° window. Due to the small-scale nature of these regions, heatwaves cannot be detected there. This can be well observed on the scattered islands off the Greek and Turkish coasts.

A heatwave minimum is located in the alpine parts and in the foothills of the Alps in Austria. Almost the whole of Hungary, together with the north-western part of Romania, is a heatwave hotspot that stands out from its neighbouring countries; only at the western end of the country, near the Austrian border, a moderate number of heatwaves per grid point can be found. This could be due to the flatness of the region, which favours the unhindered propagation of heatwaves. Like the Alps, the Carpathians are an obstacle to the spread of large heatwaves. In the parts of Serbia, Romania and Ukraine where they are located, a significant smaller number of heatwaves per grid point can be found. A larger number of heatwaves, similar in size to the heatwave hotspots in Western Europe, can be found in the mainland of Turkey, in Macedonia, northern Greece, between the borders of Romania and Bulgaria, and over central Poland. A high number of heatwaves per grid point can be seen throughout the Eastern European Plain. The Eastern European Plane includes here eastern Poland, the Ukraine, Belarus and a small part of Lithuania. The highest numbers are found in the Ukraine around Kiev and in north-eastern Belarus.

In summary, in this Eastern European region the differences between mountainous and flat landscapes have a major impact on large-scale heat waves. The differences caused by the topography can be well observed in the number of heatwaves per grid point.

4.2.4. Northern Europe

The number of heatwaves in Northern Europe in MJJASO has doubled between 1979 and 2022, see Figure 4.9a. This is a smaller increase than in Western and Eastern Europe. Nevertheless, the number of heatwave days has increased significantly, which can be at least partly attributed to the ongoing anthropogenic climate change (Bednar-Friedl et al., 2022). The smaller but still alarming increase can be partly explained by the fact that the number of heatwave days per year was already higher than in the other regions at the beginning of the observation period, with 30 days in 1979.

The spatial distribution of heatwave numbers is shown in Figure 4.9b. In Denmark only a small number of heatwaves were detected, as the country is small and surrounded by the sea. Thus, this analysis, with a defined minimum extent of grid points and without consideration of sea grid points, does not give reliable results along the coasts.

A large heatwave hotspot can be found at the southern border between Norway and Sweden. In the Stockholm region, there are many large fjords that extent far inland, so the heatwave count here is quite low and partly zero. Otherwise, almost the whole inland of Sweden and Finland has a high heatwave occurrence, comparable to the heatwave regions in central France and Germany in the Western European region. In Norway a low number is detected, except for the large heatwave area around Oslo near the Swedish border. This is partly because the country is narrow and close to the sea, but also because the Scandinavian mountain range runs through most of the country. The Northern European region also includes Latvia, Lithuania and Estonia, and a small part of Russia. They are part of the Eastern European Plane, and the number of heatwaves per grid point in these countries is very high, as it is in Eastern Europe. Finland also belongs to this plane, but the number of heatwaves is not as high as in the Baltic countries.

4.2.5. Austria

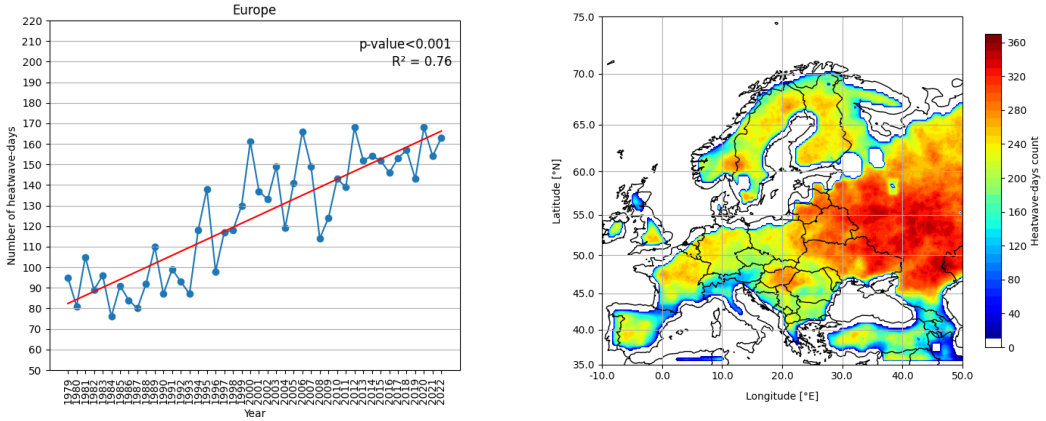
In the Figures 4.10 and 4.11 Austrian heatwaves are presented, once without and once with the condition that a heatwave must have a minimum spatial extent of 2°x2°, respectively. There are large differences between the two results. With the spatial constraint far less heatwaves were detected. Nevertheless, the number of heatwave days over time tripled in both cases, regardless of the spatial extent condition (Figure 4.10a and 4.11a). This

increase is thus a remarkable result and shows that the number of heatwave days is increasing rapidly, regardless of whether the heatwaves are small-scale or large-scale.

Depending on the detection method, there is a large difference in the location of these heatwaves in Austria. Without spatial restrictions, heatwaves occur mainly in the south of Austria, which is also south of the main ridge of the Alps. In the alpine regions a moderate heatwave count was detected. The lowest counts per grid point were found in northern Austria, i.e. in Salzburg, Upper Austria, Lower Austria, and Vienna, see Figure 4.10b. It should be noted, however, that this lower number is still higher than the maximum number of heatwaves in Austria detected with the additional spatial extent condition.

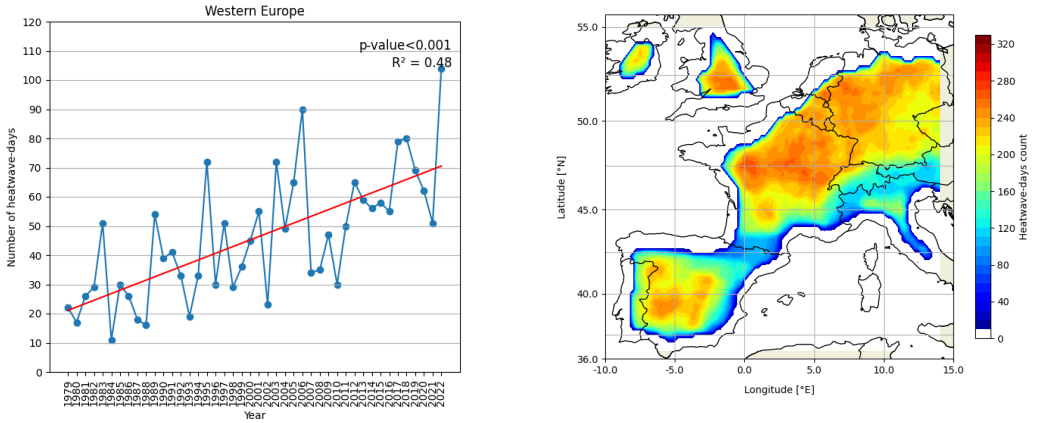
If the number of heatwaves per grid point gets assessed with the spatial extent condition, a completely different picture results, see Figure 4.11b. The areas with the highest numbers per grid point shift significantly; they are located in the upper part of Austria, i.e. the northern part of Upper Austria, Lower Austria, Vienna and Burgenland. The highest numbers are found outside the country's borders, in Bavaria, Germany, which is within the spatial range of this analysis. A minimum can be found in Salzburg. For the alpine part of Austria, but also for southern Austria the number of heatwaves per grid point is similar low. This result is consistent with the assumption that the Alps could prevent the occurrence of large-scale heatwaves; they act as a boundary. Instead, there are small-scale weather phenomena in these regions, and the occurrence of heatwaves is a local phenomenon that can vary from valley to valley. In regions where there are no geographical barriers such as mountain ranges, the number of heatwaves per grid point is higher.

When investigating a potential connection between double jet events and heatwaves in Austria, this result indicates that it is more meaningful to consider heatwaves that cover a minimum area of 2°x2° for further analysis. As seen here, without this condition many grid points with only local heatwaves were found. Double jets, however, are large-scale atmospheric phenomena that affect not only individual grid points, but a large geographical area.



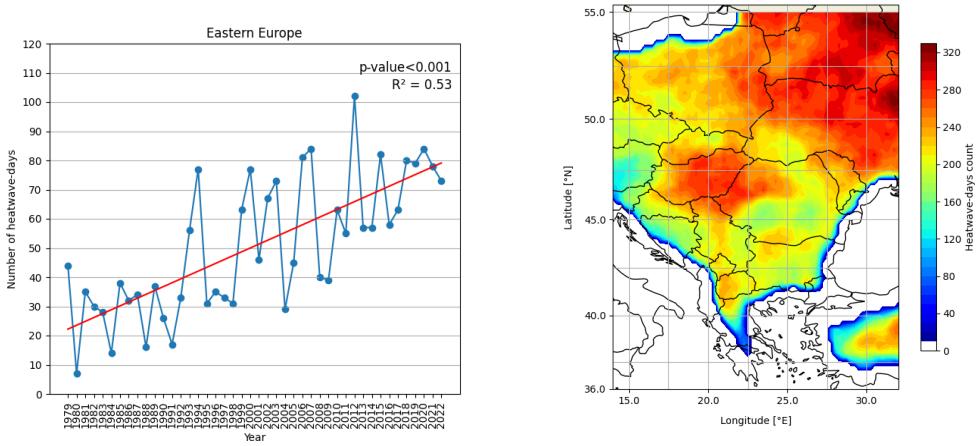
a) b)

Figure 4.6.: Heatwave days per half-year (MJJASO) from 1979 to 2022 in Europe. Panel **a** shows the count of heatwave days per year with a linear fit (red line). The associated statistically significant p-value (<0.001) and the R^2-value are shown. Panel **b** shows the number of grid points that experienced a heatwave in this period. The white areas emerge from the rolling window that was used to detect heatwaves. Since only the land grid points were used, the data availability stops at the land-ocean borders. Therefore, in these areas no heatwaves could be detected.



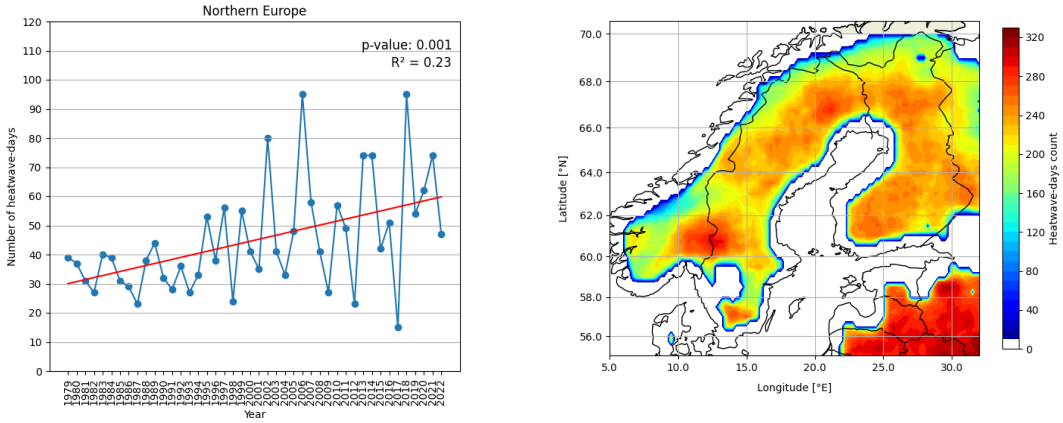
a) b)

Figure 4.7.: Heatwave days per half-year (MJJASO) from 1979 to 2022 in Western Europe. Panel **a** shows the count of heatwave days per half-year with a linear fit (red line). The associated statistically significant p-value (<0.001) and the R^2-value are shown. Panel **b** shows the number of grid points that experienced a heatwave in this period. The white areas emerge from the rolling window that was used to detect heatwaves. Since only the land grid points were used, the data availability stops at the land-ocean borders. Therefore, in these areas no heatwaves could be detected.



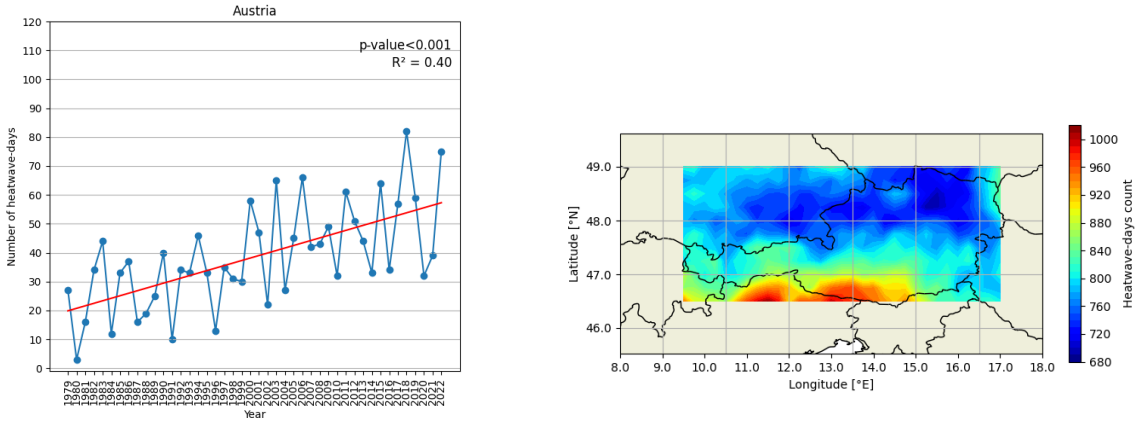
a) b)

Figure 4.8.: Heatwave days per half-year (MJJASO) from 1979 to 2022 in Western Europe. Panel **a** shows the count of heatwave days per half-year with a linear fit (red line). The associated statistically significant p-value (<0.001) and the R^2-value are shown. Panel **b** shows the number of grid points that experienced a heatwave in this period. The white areas emerge from the rolling window that was used to detect heatwaves. Since only the land grid points were used, the data availability stops at the land-ocean borders. Therefore, in these areas no heatwaves could be detected.



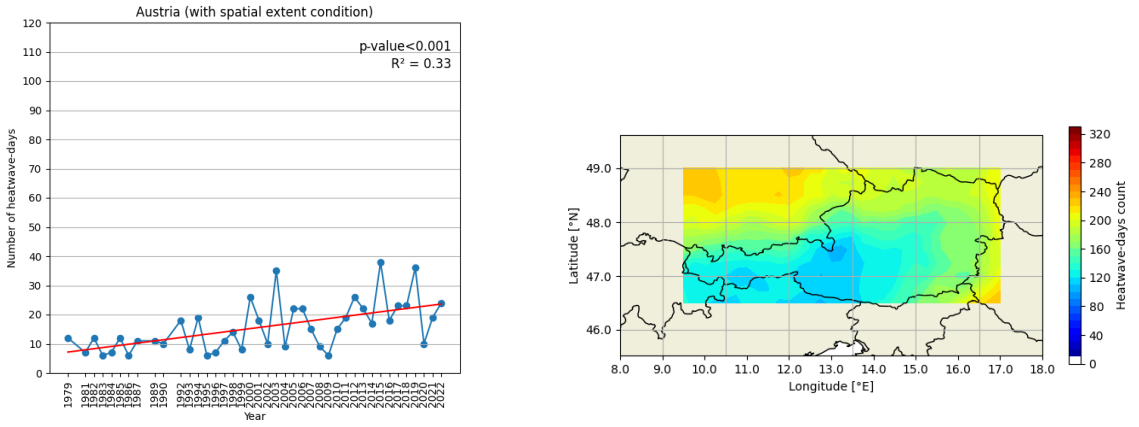
a) b)

Figure 4.9.: Heatwave days per half-year (MJJASO) from 1979 to 2022 in Northern Europe. Panel **a** shows the count of heatwave days per half-year with a linear fit (red line). The associated statistically significant p-value (<0.001) and the R^2-value are shown. Panel **b** shows the number of grid points that experienced a heatwave in this period. The white areas emerge from the rolling window that was used to detect heatwaves. Since only the land grid points were used, the data availability stops at the land-ocean borders. Therefore, in these areas no heatwaves could be detected.



a) b)

Figure 4.10.: Heatwave days per half-year (MJJASO) from 1979 to 2022 in Austria without the spatial extent condition for heatwave detection. Panel **a** shows the count of heatwave days per half-year with a linear fit (red line). The associated statistically significant p-value (<0.001) and the R^2-value are shown. Panel **b** shows the number of grid points that experienced a heatwave in this period. Due to the large difference in the number of grid points in contrast to the analysis of Austria with the spatial extent condition (see Figure 4.11b), the color scale is different.



a) b)

Figure 4.11.: Heatwave days per half-year (MJJASO) from 1979 to 2022 in Austria with the spatial extent condition (a heatwave must cover at least 90 percent of all grid points in a 2°x2° window around the central grid point). Panel **a** shows the count of heatwave days per half-year with a linear fit (red line). The associated statistically significant p-value (<0.001) and the R^2-value are shown. Panel **b** shows the number of grid points that experienced a heatwave in this period. The color scale is different in contrast to the analysis of Austria with small-scale heatwaves (see Figure 4.10b) since here way lower heatwave numbers are detected.

4.3. Connection of Double Jet Events and Heatwaves

4.3.1. Results Monte-Carlo Analysis

The results of the Monte-Carlo test are shown in Table 4.1. A total of 2339 double jet days were found in the months MJJASO for the whole period from 1979 to 2022. This number served as the number of days randomly drawn from the whole period for the individual runs of the Monte-Carlo analysis. The number of days on which both a double jet and a heatwave occurred varies from region to region. For Austria, *without* the spatial extent condition for a heatwave, 467 days were found. The frequency of the occurrence of a heatwave in the presence of a double jet was 19.97 percent. For Austria, *with* the spatial extent condition for a heatwave, the number of days is significantly smaller, the frequency of a heatwave occurrence with a double jet present is thus at only 7.84 percent.

For Western Europe, 622 days with both a heatwave and a double jet were found; the frequency of the observed heatwaves when a double jet was present is at 26.25 percent. For the Eastern European region, the number of days for a simultaneous occurrence of double jets and heatwaves is even higher than for Western Europe, although the spatial extent is slightly smaller. However, the number of heatwaves is generally higher in this region. Therefore, the frequency of heatwaves occurring when a double jet is present is also higher in Eastern Europe, at 29.41 percent. The highest frequency of 40.14 percent was calculated for Northern Europe, where the number of heatwave and double jet days is by far the highest, with 939 days recorded in MJJASO from 1979 to 2022.

In the table, the higher heatwave frequency is highlighted for days with a double jet compared to randomly selected days for each region. In Western Europe, the heatwave frequency with a double jet present is higher than the 90th percentile of the heatwave frequencies detected from the Monte-Carlo analysis with 500 runs. The same is true for Eastern Europe and Northern Europe. In these regions double jets could indeed have a connection to heatwaves. This does not apply to Austria, regardless of whether the spatial extent condition was used for the heatwave detection. The heatwave frequencies when a double jet is present are even close to the 10th percentile of the random heatwave frequencies, see Figure 4.12. Therefore, no statistically significant connection between heatwaves and double jets could be detected for the region of Austria. This suggests that either Austria may be too small in size to be associated with such large-scale events like double jets, or that there is in fact no link between heatwaves in Austria and double jet events.

Comparing the numbers of the heatwave frequencies in the presence of a double jet with the frequencies for random days, it is striking that they are

very similar. For Western Europe, where a significant connection between heatwave and double jet occurrence could be found, the difference is only at 0.0072. The difference in frequencies in the other regions is slightly larger but still very small, except for Northern Europe where there is a substantial difference. Nevertheless, the distribution ranges of the random heatwave frequencies from the 500 the Monte-Carlo runs are very close together, as can be seen in Figure 4.12.

For Western Europe the distribution range is from approximately 0.23 to 0.27. This small range makes the difference in frequencies appear more significant; the frequency of heatwaves in the presence of a double jet is almost at the very end of the distribution curve.

This is similar for Eastern Europe. The distribution ranges from 0.25 to approximately 0.29, with the heatwave frequency in the presence of a double jet at the very end of this range.

For Austria, the two distribution plots show a similar pattern, regardless of the heatwave detection method used, even though the distribution ranges are at different scales. In both cases, the heatwave frequency in the presence of a double jet is far behind the majority of the random distribution values, at the lower end of the distribution curve. Therefore, based on this analysis, a significant correlation between heatwaves and double jets could not be established for Austria.

Northern Europe is a special case. Here, the distribution range is from approximately 0.22 to 0.27, but the heatwave frequency with a double jet present is at 0.40. This is far outside of the distribution range. This result suggests a highly statistically significant connection between heatwaves and double jet events in Northern Europe.

Table 4.1.: Results of the Monte-Carlo analysis. The bold numbers highlight for each region the higher heatwave occurrence frequency between the frequency when a double jet is present and the frequency on randomly selected days.

Regions	**Double jet- and heatwave-days**	**Frequency of heatwave-occurrence when double jet is present**	**90th percentile for random days (n=500)**	**50th percentile for random days (n=500)**
Austria	467 days	0.1997	**0.2180**	0.2095
Austria (with spatial extent condition)	175 days	0.0784	**0.0855**	0.0799
Western Europe	622 days	**0.2659**	0.2587	0.2493
Eastern Europe	688 days	**0.2941**	0.2860	0.2753
Northern Europe	939 days	**0.4015**	0.2536	0.2437

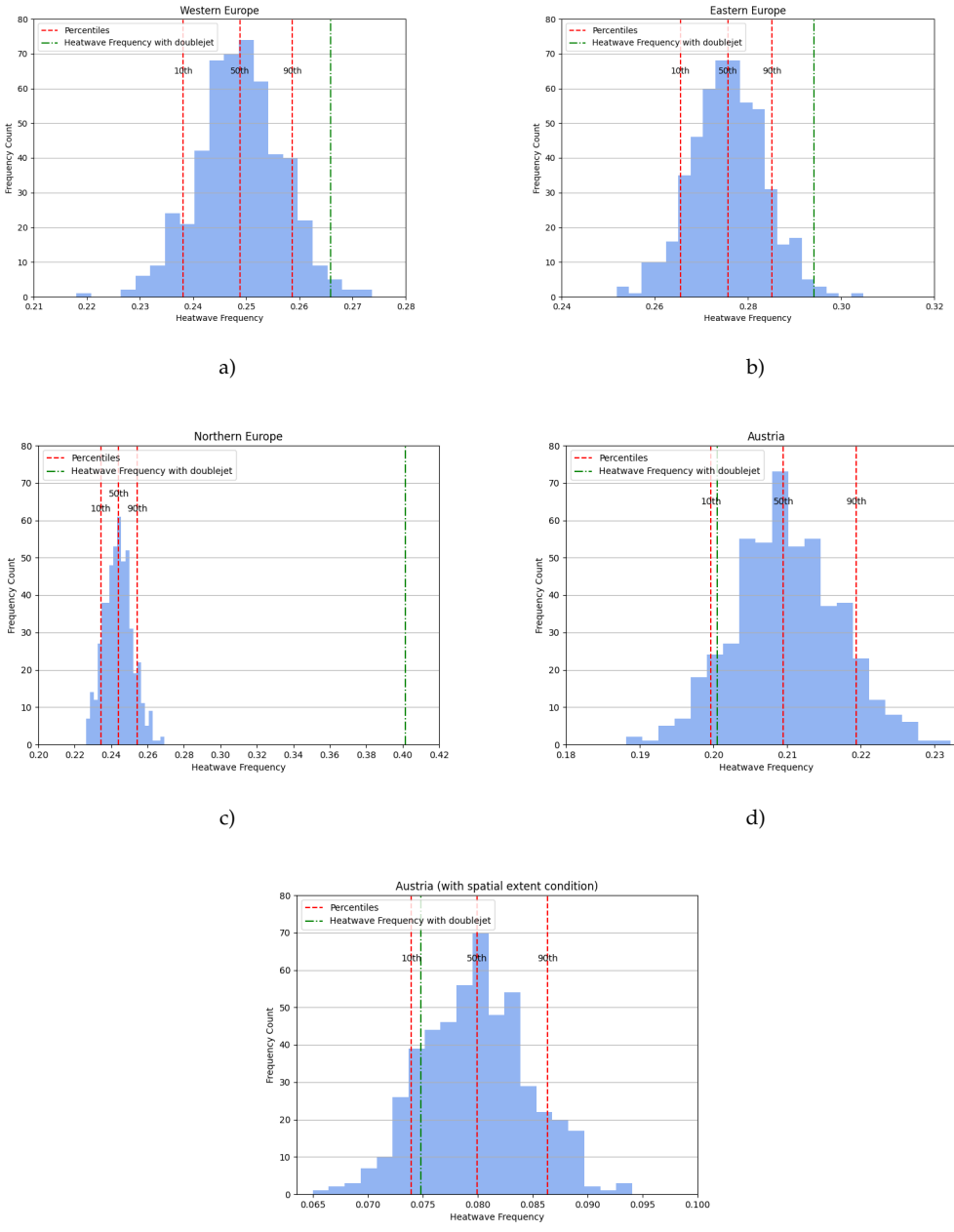


Figure 4.12.: Distribution of the random heatwave frequencies for Western Europe (Panel **a**), Eastern Europe (Panel **b**), Northern Europe (Panel **c**), Austria (Panel **d**), and Austria with the spatial condition for heatwaves (Panel **e**). The 10th, 50th, and 90th percentiles (red lines) and the heatwave frequency when a double jet is present (green line) are shown in each panel.

4.3.2. Linear Correlation between Double Jets and Heatwaves

Figure 4.13b shows the number of days per half-year (MJJASO) on which both a double jet and a heatwave occurred for Western Europe. A statistically significant increase (p=0.01) of 10 days could be found over the analysed period from 1979 to 2022. From this result alone, one might assume that there is a clear connection between double jets and heatwaves, and that this connection gets more pronounced in recent years. However, this is not so easy to determine as a look at Figure 4.13b reveals. Here, the separate counts of double jet days per year and heatwave days per year with the corresponding regression lines can be seen. While the number of double jet days per year fluctuates but does not increase over time, the number of heatwave days per year increases significantly, as discussed in previous sections. Therefore, it can be assumed that the increase in the number of days on which both a double jet and a heatwave occur is solely due to the large increase in the number of heatwave days per year. Although it is possible that some heatwave days are due to the presence of a double jet event, it is more likely that the observed increase in the number of heatwave and double jet days over time is due to random coincidences caused by the increase in heatwaves. A statement about the correlation between double jet days and heatwave days is not possible with such a simple analysis, as shown here for the western European region as example.

In order to assess a potential correlation between jet streams and heatwaves, both data series were detrended. Pearson's correlation coefficient was then calculated. For Western Europe a correlation coefficient of 0.09 was found, see Figure 4.14. This number is very close to zero and means that basically no linear correlation could be found. The p-value is also above the significance level.

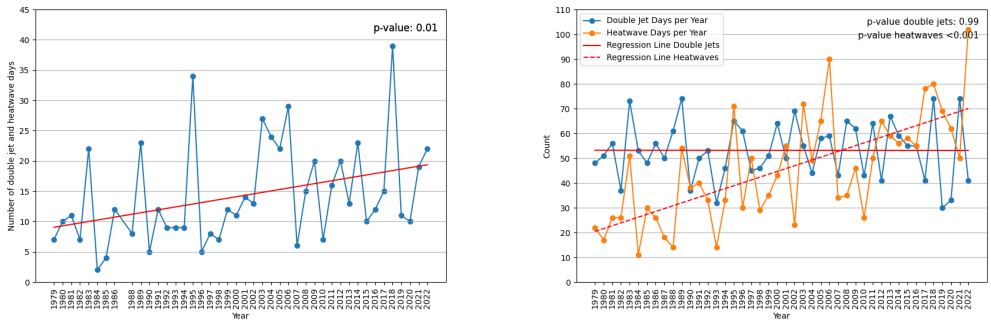
In Figure 4.15 a correlation coefficient of -0.14 and a p-value of 0.38 were calculated for Eastern Europe. As before, no statistically significant correlation was found.

For Northern Europe a correlation coefficient of 0.47 and a p-value of 0.001 were calculated. This correlation value indicates a positive correlation, the result is also statistically significant.

In Figure 4.17 the correlation analysis for Austria, with and without the spatial extent condition for the heatwave detection, is displayed. In both cases, Pearson's correlation coefficient is close to zero and the p-value is above the significance level. Therefore, no significant linear correlation between heatwave days and double jet days could be found for Austria.

However, even though a positive linear correlation could only be detected for Northern Europe, this does not mean that there could not be another non-linear correlation in the other regions. If many other factors would

influence the occurrence of heatwaves in the other regions, the influence of a double jet stream event could not be determined with a simple linear correlation.



a) b)

Figure 4.13.: Panel **(a)** shows the number of days per half-year (MJJASO) from 1979 to 2022 when a double jet event and a heatwave occurred in Western Europe, together with a linear fit (red line). Also the associated p-value is shown. In Panel **(b)** the half-yearly counts of double jet days and heatwave days with their respective linear fits (red line for double jet days, dashed red line for heatwave days) and their associated p-values are shown separately.

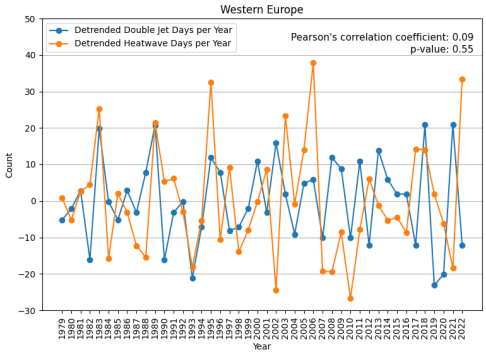


Figure 4.14.: Correlation between detrended double jet days (blue line) and heatwave days (orange line) per half-year (MJJASO) in Western Europe, with the associated Pearson's correlation coefficient and the p-value.

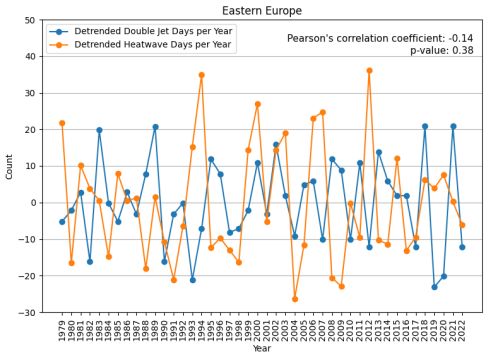


Figure 4.15.: Correlation between detrended double jet days (blue line) and heatwave days (orange line) per half-year (MJJASO) in Eastern Europe, with the associated Pearson's correlation coefficient and the p-value.

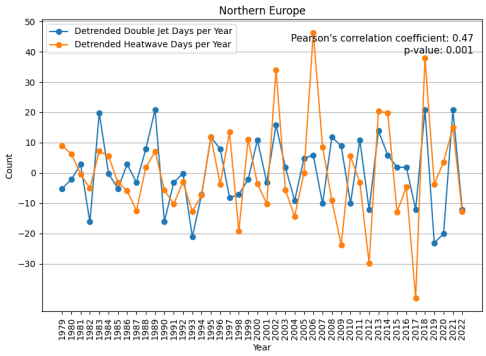
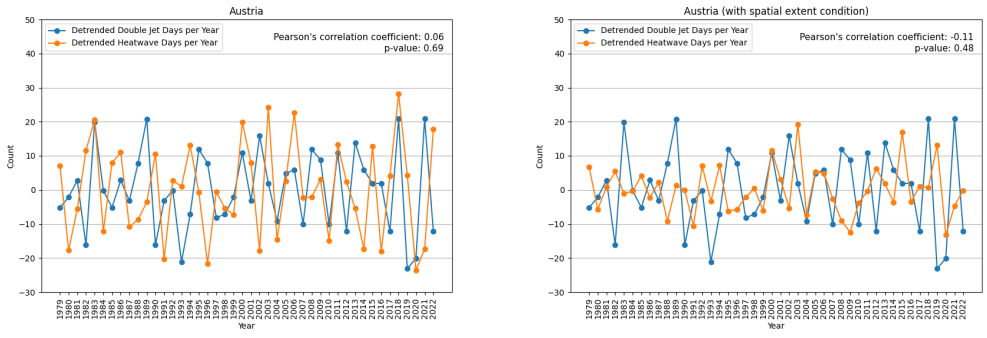


Figure 4.16.: Correlation between detrended double jet days (blue line) and heatwave days (orange line) per half-year (MJJASO) in Northern Europe, with the associated Pearson's correlation coefficient and the p-value.



a) b)

Figure 4.17.: Correlation between detrended double jet days (blue line) and heatwave days (orange line) per half-year (MJJASO) with the associated Pearson's correlation coefficient and the p-value for Austria (Panel **a**), and for Austria with the spatial extent condition for the heatwave detection (Panel **b**).

4.3.3. Spatial Impact of the Double Jet Stream on Heatwaves in Europe

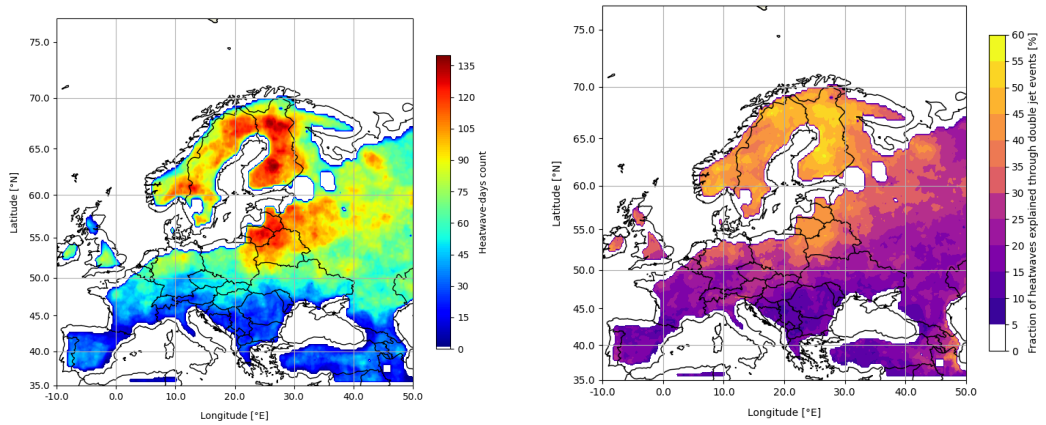


Figure 4.18.: European heatwaves coinciding with double jet events. Panel **a** shows the number of heatwaves per grid point that can be attributed to a double jet event. Panel **b** shows the percentage of heatwaves that can be attributed to a double jet event.

In Figure 4.18a the number of heatwaves per grid point that can be attributed to a double jet event is illustrated. In the northern part of Europe, from approximately 50°N northwards, the number of heatwaves is significantly higher. Particularly high numbers are found in the Nordic and Baltic countries. In the southern part of Europe, south of 50°N, there are only small numbers of heatwaves detected that can be associated with a double jet event, even though the total number of heatwave days in some regions, such as central Spain, central Turkey or Hungary, is as high or even higher than in northern Germany, for example, where the correlation is more pronounced (see Figure 4.6b). This indicates that double jets exert their main impact in the northern part of Europe, while heatwaves in other parts of Europe are caused by other influences. This is not surprising, since the jet stream is often present over Northern Europe. Also, according to the definition of a double jet, the area enclosed by two branches of the jet in a double jet event is located between 45° and 65°N. The high number of heatwave days in Russia and Ukraine is also not reflected. This means that these heatwaves also have other causes and influences. It is also possible that the restriction of double jet detection to Europe plays a role, and that double jets over Asia could still be correlated with these heatwaves.

The percentage of heatwaves that can be attributed to a double jet event out of the total heatwaves per grid point is shown in Figure 4.18b. In general, the

percentage distribution follows the spatial pattern of the detected heatwaves associated with a double jet event. While the proportion of heatwave days linked to a double jet is only between 5 and 25 percent in southern parts of Europe, it rises up to 60 percent in the Nordic countries and the Baltic region. In regions where the double jet has a strong effect, it coincides with almost half or even more of all large-scale heatwaves. Nevertheless, also in some other regions a stronger influence of the jet stream can be observed. An interesting example is Austria. Here, only a small number of heatwave days can be attributed to a double jet event (see Figure 4.18a), and the total number of large-scale heatwaves is also small (see Figure 4.11b). However, of this small number of large-scale heatwaves in the eastern, non-alpine region of Austria, between 25 and 30 percent can be related to a double jet event.

4.3.4. Persistent Double Jet Events and Severe Heatwaves

For Western Europe, the linear fit in Figure 4.19a shows a slight increase, but no statistically significant trend can be found (p-value = 0.092). No connection between double jet event duration and heatwave severity can be detected. Most of the heatwaves can be connected to double jet events with a persistence between 3 and 10 days. Only a few heatwaves can be linked to longer double-jet events. The number of heatwaves per grid point that can be attributed to a double jet event (Figure 4.19b) is low over the whole southern part of Western Europe. This includes the centre of the Iberian Peninsula, where a heatwave hotspot was found in the analysis of the large-scale heatwaves per grid point for Western Europe (Figure 4.7b). This hotspot could not be related to persistent double jet events. In mountainous regions, i.e. the Alps and the Pyrenees the number of heatwaves per grid point is particularly low. The maximum numbers of heatwaves are located in the northern part of Germany, Ireland, and the UK. The maximum number of heatwaves for the Western European region is lower than in the analysis of heatwaves conducted for the whole European region, see Figure 4.18a. This may be due to the overlapping of heatwaves, as described in the methodology (see Section 3.2.4). However, in general the spatial distribution pattern of the two analyses is consistent.

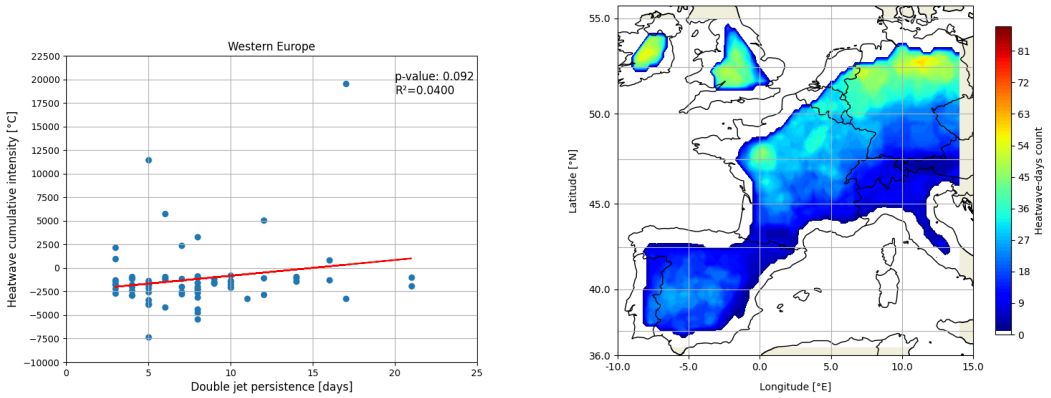
For Eastern Europe (4.20a) the p-value does not indicate a statistically significant result (p-value = 0.504). Most heatwaves that can be connected to a double jet were found for a double jet duration between 3 and 13 days. For longer double jet durations, only few associated heatwaves can be detected. The spatial distribution of the number of heatwaves per grid point that can be connected to a double jet event is shown in Figure 4.20b. The spatial distribution pattern is consistent with the same analysis for the whole European region (Figure 4.18a).

Throughout the southern part of the subregion only few heatwaves can

be attributed to a double jet event. In areas where there are fewer heatwaves to begin with, such as over the Carpathians, the number is even lower. From about 50°N northwards the number of heatwaves per grid point increases. However, the highest numbers of heatwaves attributed to double jets are not located at the locations where the highest heatwave numbers in the total heatwave analysis could be found (see Figure 4.8b). A heatwave hotspot was located throughout Hungary, northwestern Romania, and parts of the Czech Republic. This hotspot cannot be detected in Figure 4.20a, meaning that heatwaves in that area could not be connected to a double jet event. Also in the analysis of the spatial impact of the double jet stream on heatwaves for the whole region of Europe this hotspot was not detected (Figure 4.18a). This indicates, that the double jet stream actually has very little influence in this area and that a greater influence can only be detected from 50°N northwards.

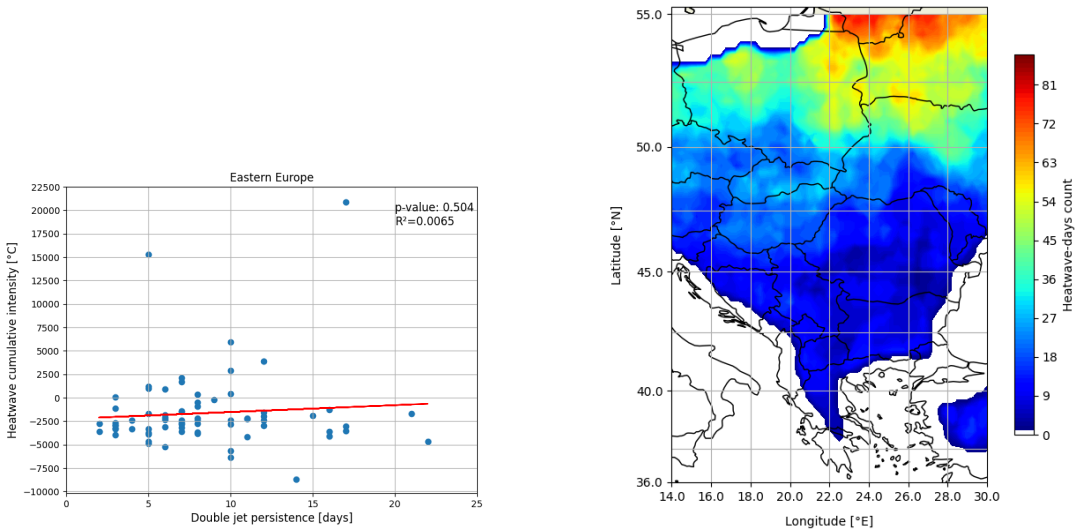
For the Northern European region, a statistically significant increase in the heatwave cumulative intensity with more persistent double jet events can be observed, see Figure 4.21a. Most heatwaves connected to a double jet event are found for double jet durations between 3 and 15 days. The heatwave cumulative intensity increases as the event duration increases; this increase is statistically significant (p-value$<$0.001). This result shows that more persistent double jet events are associated with more severe heatwaves with a higher cumulative intensity in Northern Europe. The spatial distribution of the heatwaves that can be connected to a double jet event is shown in Figure 4.21b. Also for Northern Europe this spatial distribution pattern is consistent with the pattern of the same analysis for the whole European region (Figure 4.18a). In northern Sweden and especially in northern Finland maximum numbers of heatwave days per grid point that can be attributed to a double jet event are located. Also in Estonia, Lithuania, and Latvia the number of heatwaves per grid point is high. In the western part of Russia the number is lower, even tough the detected total number of heatwaves is as large as in the Baltic countries (Figure 4.9b).

The overall number of heatwaves associated with a double jet is much higher in Northern Europe than in Western Europe (Figure 4.19a) and also in most of Eastern Europe (Figure 4.20a). The influence of double jet events on heatwaves thus appears to be greatest at higher latitudes.



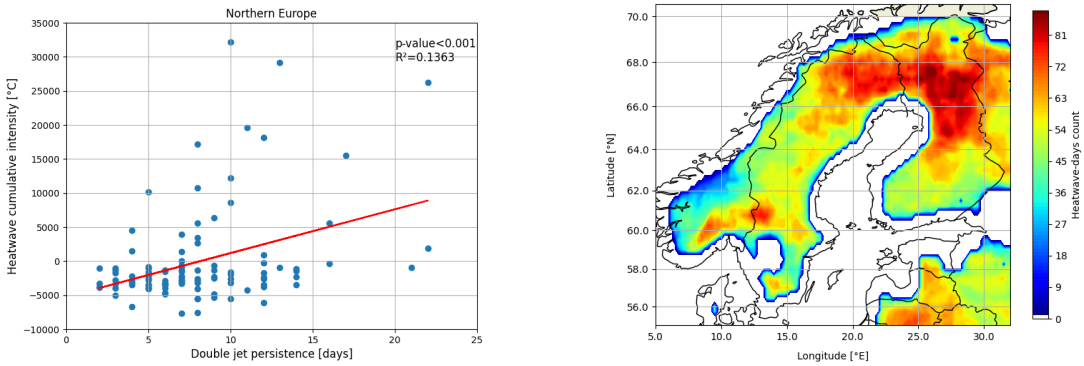
a) b)

Figure 4.19.: Double jet persistence and heatwave cumulative intensity for Western Europe. Panel **a** shows the scatter plot of the double jet event durations with the detrended heatwave cumulative intensities together with a linear fit (red line, not statistically significant). Panel **b** shows the spatial distribution of the heatwaves that can be attributed to a double jet.



a) b)

Figure 4.20.: Double jet persistence and heatwave cumulative intensity for Eastern Europe. Panel **a** shows the scatter plot of the double jet event durations with the detrended heatwave cumulative intensities together with a linear fit (red line, not statistically significant). Panel **b** shows the spatial distribution of the heatwaves that can be attributed to a double jet.



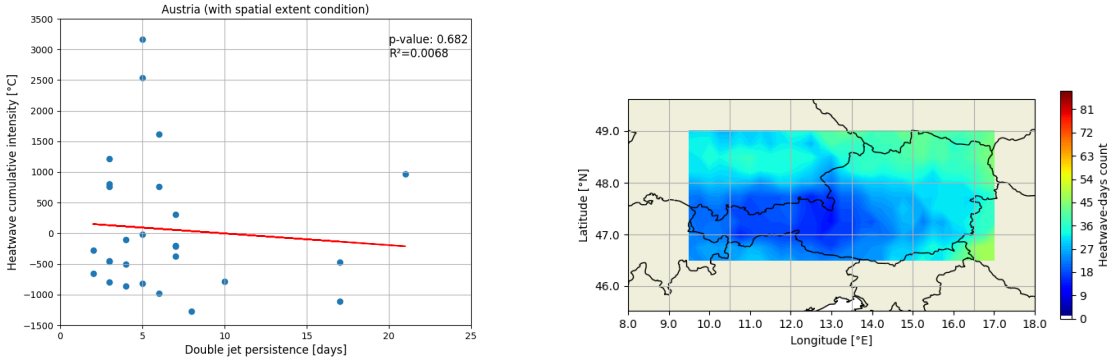
a) b)

Figure 4.21.: Double jet persistence and heatwave cumulative intensity for Northern Europe. Panel **a** shows the scatter plot of the double jet event durations with the detrended heatwave cumulative intensities together with a linear fit (red line, statistically significant, p-value<0.001). Panel **b** shows the spatial distribution of the heatwaves that can be attributed to a double jet.

For Austria, with the spatial extent condition for heatwave detection, only a few heatwaves could be associated with a double jet stream event. These few data points are also widely scattered, as can be seen in Figure 4.22a. Therefore, no linear relationship could be found between persistent double jet events and the cumulative intensity of a heatwave. The regression analysis even shows a decrease in intensity with more persistent events, but the result is not statistically significant. As only a few heatwaves could be attributed to persistent double jet events, the number of heatwave days per grid point that can be connected with a double jet is low (Figure 4.22b). For the whole western part of Austria the number is particularly low. Only in the upper part of Austria, i.e. in Vienna, and in upper parts of Lower Austria and Upper Austria, the number increases to a moderate level. This spatial distribution pattern is consistent with the pattern of the same analysis for the whole European region (Figure 4.18a).

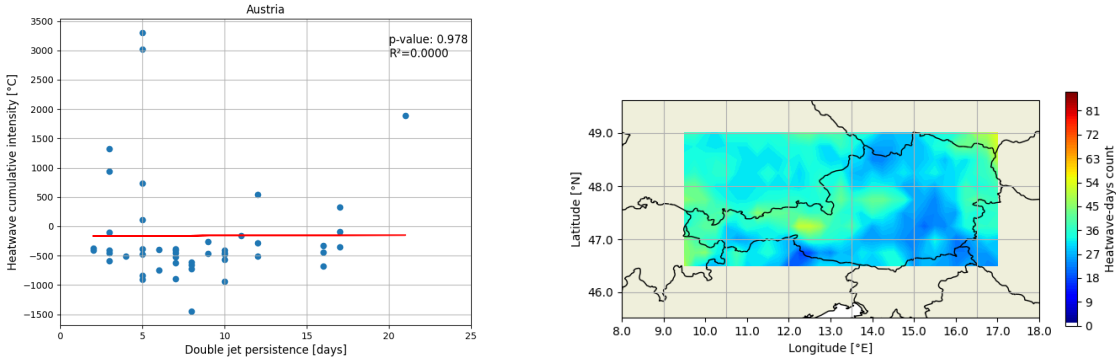
For Austria, without the spatial extent condition for heatwave detection, the detected overlap between heatwaves and double jet events is not as scattered as for Austria with the spatial extent condition. However, again there is no increase in heatwave intensity with increasing duration of double jet events. No connection between more persistent double jet events and higher heatwave cumulative intensity can be established, see Figure 4.23a. The local distribution of these heatwaves associated with a double jet appears to be arbitrary, see Figure 4.23b. A maximum is found for alpine regions where previous (Figure 4.18) no influence of a double jet event could be detected. There is also no similarity to the pattern of the total detected

heatwaves (Figure 4.10b). Therefore, it can be assumed that the matches between heatwaves and double jet events in this analysis are due to chance.



a) b)

Figure 4.22.: Double jet persistence and heatwave cumulative intensity for Austria with the spatial condition for the heatwave detection. Austria with small-scale heatwaves is depicted in Figure 4.23. Panel **a** shows the scatter plot of the double jet event durations with the detrended heatwave cumulative intensities together with a linear fit (red line, not statistically significant). Panel **b** shows the spatial distribution of the heatwaves that can be attributed to a double jet.



a) b)

Figure 4.23.: Double jet persistence and heatwave cumulative intensity for Austria with small-scale heatwaves. Austria with large-scale heatwaves is depicted in Figure 4.22. Panel **a** shows the scatter plot of the double jet event durations with the detrended heatwave cumulative intensities together with a linear fit (red line, not statistically significant). Panel **b** shows the spatial distribution of the heatwaves that can be attributed to a double jet.

The months, in which heatwaves that could be explained by a double jet event occurred, are displayed in Figure 4.24. The pattern of the monthly occurrence of heatwaves across the entire European region is similar to that of the subregions and Austria. Lower numbers were found for August, September, and October, while the highest number of occurrence is found for June, followed by May and July. The lowest number of heatwaves in Western Europe, Eastern Europe and Austria occurred in August. A high number of heatwaves in Western and Eastern Europe were recorded in May and June, while in Austria the highest number was recorded in October, followed by June. In Northern Europe the number of heatwaves that can be connected to a double jet is generally higher, with June again being the most frequent month, followed by July and May. September and October are here the months with the fewest occurrences.

This is fairly consistent with the general occurrence of double jet streams throughout the observed period, see Figure 4.2b. The highest number of double jet stream states occurred in June and the lowest number in August. Thus, a higher number of double jet days could be directly related or responsible for a higher number of heatwave days. It is also evident from these graphs, that the effects of the double jet are most pronounced at more northerly latitudes.

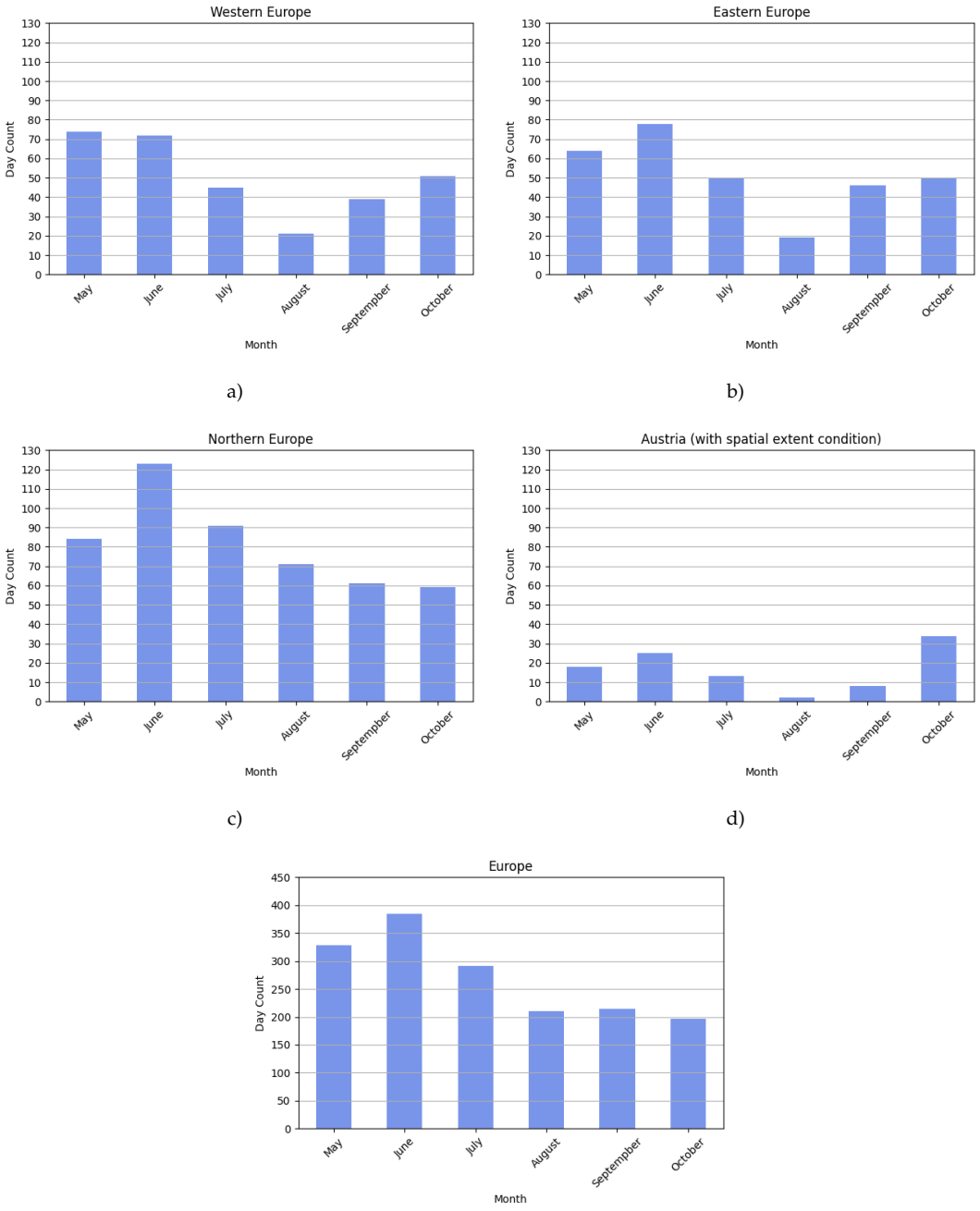


Figure 4.24.: Monthly occurrence of heatwaves that can be attributed to a double jet stream event, based on analysing the heatwave cumulative intensity and persistent double jets for Western Europe (Panel **a**), Eastern Europe (Panel **b**), Northern Europe (Panel **c**), and Austria with the spatial extent condition for heatwaves (Panel **d**). Panel **e** shows the monthly occurrence of heatwaves that can be attributed to a double jet stream for Europe, based on analyzing composites of heatwaves and persistent double jets per grid point. Heatwaves are always attributed to the month they begin in.

5. Discussion

5.1. Double Jet Stream Frequency

On average, a double jet stream frequency of almost 30 percent was found for MJJASO over the period from 1979 to 2022. This is approximately in agreement with the findings of Rousi et al. (2022a), see Chapter 4.1.1. The monthly mean frequency of the double jet stream for the period 1979 to 2022 is 20 percent for August, which is the lowest frequency for the analysed months MJJASO (see Figure 4.2b). This is in contrast to the analysis of Rousi et al. (2022a), who found a double jet mean frequency of 36 percent in July and August for the period 1979 to 2020. A possible explanation for this discrepancy are the different geographical regions studied, which makes the frequencies of these two analyses not comparable. They assessed double jet stream states over the Eurasian area, while in this thesis the European area was analysed. Nevertheless, this could indicate that there is a higher frequency of double jets over Asia in July and August.

5.2. Altitude and Latitude of the Double Jet Stream

The altitude and latitude of the double jet peaks varied considerably over the period 1979 to 2022 (see Figures A.1 and A.2). Over time, no trend in the location of the double jet towards higher or lower altitudes or latitudes emerged. What can be observed is a clear separation of the two branches of the double jet stream. The branch that is regarded as the subtropical jet stream stretches between an altitude of around 11.000 to 13.000 metres. 13.000 metres is the upper end of the chosen range of the analysis. The latitudinal position lies between 20°N and 50°N. The branch that is regarded as the polar jet stream ranges between an altitude of 8.000 to 11.000 metres and lies between a latitude of around 60°N to 80°N. 80°N is the maximum latitude of the chosen range of the analysis. Some of the detected double jet peaks in both jets are located at the boundaries of the altitude and latitude ranges analysed. To map a even more precise location of each double jet state, these boundaries could be extended, however, the jet is considered to be already sufficiently represented in this work. The clear separation shows

that the double jet detection algorithm has worked successfully and that the definition of the double jet is reasonable.

5.3. Variability of the Longest Double Jet Event per Year

The analysis of the variance of the longest double jet event per half-year showed much stronger fluctuations over the last decade than in the three decades before (see Figure 4.5). This suggests that the longest events in each year vary considerably in their event duration. A possible reason for the discontinuity in event durations could be a change in atmospheric dynamics and the associated change in circulation patterns. At present, however, there are no significant trends indicating a more variable atmospheric circulation in the Northern Hemisphere or a higher variability of the jet stream. What can be observed are seasonal and regional variations in Rossby wave amplitude and velocity, but these are within the range of natural variability (Fragkoulidis, 2022).

One reason for the difficulty in capturing changes and distinguishing them from natural variability could be the tug-of-war between Arctic amplification and tropical upper tropospheric warming discussed in Chapter 2.3. These two mechanisms exert opposing effects on the jet stream and thus modulate each other which results in a weaker overall effect. Nevertheless, driven by the ongoing climate change due to anthropogenic emissions, a trend could emerge out of natural variability in the coming years due to a higher tropical upper tropospheric warming which is thought to have a stronger effect on the jet stream. Therefore, further research is needed to better understand the effects of this particular mechanism (Woollings et al., 2023). Such an emerging trend could potentially help to explain the fluctuations in variance detected here.

In this work, however, no statistically significant difference in variance was found between two distinct groups of the longest events per year (see Figure 4.3) using Levene's test. This is also true for 3 distinct groups. However, the last decade, in which an increase in variance was found, is not well represented by this group size. A smaller group size would be required to assess this time period, but then Levene's test cannot be performed because a larger sample size is needed (Haslwanter, 2016). In the future, with more observational data and, therefore, a longer time series available, possible differences in variance may be found.

5.4. Spatial Impact of the Double Jet Stream on Heatwaves in Austria

Between 25 and 30 percent of large-scale heatwaves can be related to a double jet event in Austria (see Section 4.3.3). Thus, even though the occurrence of large-scale heatwaves in Austria is low, a quarter of them occurred at the same time as a double jet stream event. However, a statistically significant link between heatwaves in Austria and double jet events has not been found in the analyses carried out in this thesis. This could be due to the fact, that the detected number of large-scale heatwaves in Austria was too small to detect a link with the analysis methods used. Without further results indicating such a link, a connection between double jets and heatwaves cannot be established for Austria.

6. Summary and Conclusions

The jet stream has a major influence on weather patterns in the Northern Hemisphere and is, therefore, an important driver of weather extremes. Heatwaves are extreme weather events, that have become increasingly frequent in recent decades, primarily due to anthropogenic climate change; in particular, Europe has been identified as a heatwave hotspot. A so-called double jet stream possibly contributes to this increase in heatwaves. During a double jet event, the jet splits up into two branches that effectively trap weather conditions between them, potentially resulting in more persistent heatwaves. Nevertheless, the extent of the relationship between double jet streams and heatwaves remains uncertain, partly due to the limited number of studies on double jet streams themselves.

This thesis addresses this knowledge gap by developing a methodology for identifying double jet stream states over Europe and subsequently analyzing their characteristics for the extended summer period from May to October (MJJASO) from 1979 to 2022. To explore potential links, double jet streams were analysed together with heatwaves for different European regions, i.e. Western Europe, Eastern Europe, and Northern Europe. As a special case in Central Europe, the analysis was also conducted for Austria.

Double Jet Stream Variability

The number of days where a double jet stream occurred varied widely across the studied period from 1979 to 2022; between 30 and 75 double jet days per half-year (MJJASO) were found. However, no significant trend could be detected indicating an increase or decrease in double jet days in MJJASO over 1979 to 2022. The frequency varies between 20 percent to approximately 40 percent. The average frequency is at approximately 30 percent, which means that on one third of all days analysed a double jet was found. Examining the monthly distribution, the double jet frequency peaked in June, with a frequency of 37 percent, and is lowest in August, with a frequency of 20 percent.

The duration of double jet events remained relatively constant over time, showing no significant trend towards longer or shorter double jet events.

The altitude and latitude position of the detected double jets varied significantly, but no significant trend suggesting a shift in the position of the double jet could be found. This is in accordance with literature, where no trend has yet been found that can be distinguished from natural variability.

To assess the maximum length of double jet events, the longest double jet event for each year in the period MJJASO was recorded. They had an average duration of 11 days. The shortest events across all years lasted 5 days, while the longest event extended to 22 days in 2013. A substantial proportion of the longest events occurred in May, here 16 out of 43 events were recorded. June also experienced a high occurrence with 10 events, while other months featured 3 to 5 of the longest events.

When performing an Levene's test for two distinct groups of the timeline of the longest event of each year, no significant difference in variance could be found, implying no statistically significant changes in the variability of the longest event durations between the two groups. When calculating the moving variance with a 5-year, a 9-year, and a 11-year window, the moving variance remained consistent until 2008 but suddenly increased afterwards, doubling for all window sizes. This suggests that the duration of the longest double jet events per year varies stronger between long and short events in recent years. The reason for this change remains unclear. It may be linked to shifts in atmospheric circulation, but so far, no trend has been identified, that can be distinguished from natural variability.

Extended Summer Heatwaves

The number of European heatwave days in the extended summer period has increased considerably. For the total European area the number of heatwave days has more than doubled from 1979 to 2022. This trend continues when heatwave days are examined for individual subregions. For Western and Eastern Europe, the number of heatwave days has more than tripled, and for Northern Europe the number has doubled. The area with the highest number of heatwaves per grid point is located in the east of the European region, in Ukraine, western parts of Russia, and the Baltic countries. In Western Europe, there are high heatwave numbers in northern and middle France and Germany, the UK and in central Spain. In Alpine regions the number of large-scale heatwaves is low. In Eastern Europe, a heatwave hotspot around Hungary and north-western Romania is found. In Northern Europe, a high number of heatwaves per grid point is located at the southern border of Norway and Sweden. For Sweden and Finland, a high number of heatwaves was detected in general.

For Austria, both large-scale heatwaves and small-scale heatwaves were assessed, based on analysing selected large and small spatial extents. In both cases the number of heatwaves tripled over the analysed time period, however, the spatial distribution is different. In general, a way higher number of small-scale heatwaves was found. They occurred mainly south of the main ridge of the alps, while in alpine parts of the country and in the north moderate numbers were found. Large-scale heatwaves, however, are mainly located in the north and east of Austria, while the numbers that occurred in

alpine parts and the south are low.

Connection of Double Jet Events and Heatwaves

A Monte-Carlo analysis was carried out to test the significance of the connection between double jets and heatwaves. For all three European subregions, Western, Eastern, and Northern Europe, a statistically significant connection between double jet days and heatwave days could be established. For heatwaves in Austria no statistically significant connection was found, regardless if they are large-scale or small-scale.

For Northern Europe, a statistically significant (p=0.001) correlation coefficient of 0.47 was determined with Pearson's correlation. For all other regions, correlations were non-significant.

A strong connection of heatwaves and double jets events was found in the northern European region, northward of about 50°N. Especially high numbers of heatwaves, that can be connected to a double jet stream event are found for Scandinavia, the Baltic countries, and parts of Russia. High numbers were also located in the UK, northern Germany, and in Poland. In the southern part of Europe, the number of heatwaves that can be connected to a double jet event is low, even when the total number of heatwaves is similar as in regions in Northern Europe.

This spatial pattern stays the same when observing the percentage of heatwaves that could be associated with a double jet stream instead of the absolute numbers. In southern parts of Europe, the proportion of heatwave days that are related to a double jet varies between a percentage of 5 and 25 percent. In the northern parts of Europe, the percentage varies between 30 and 50 percent. In parts of Scandinavia the proportion even rises up to 60 percent. A double jet event, therefore, has a major impact on heatwaves in the northern part of Europe, while heatwaves in the southern part are often unrelated to double jets. This can be explained with the appearance of a double jet. Very often one of the branches passes at about 70°N, while the other passes at about 45°, i.e. over the southern European region. According to theory, persistent heatwaves can occur in the center of the two branches, which is the northerly part of Europe identified in this thesis as a hotspot of heatwaves that can be related to a double jet event. The monthly occurrence of the absolute number of heatwaves that can be attributed to a double jet stream approximately corresponds to the distribution of double jet days over the months. Most of these heatwaves occurred in June, followed by May and July.

Finally, a statistically significant connection between double jet event duration and heatwave severity was found for Northern Europe. The heatwave cumulative intensity rises with a longer double jet event duration. This connection cannot be established for Western Europe, Eastern Europe and Austria. Although for Western and Eastern Europe an increase in heatwave

cumulative intensity with more persistent double jet events was found, that increase is not statistically significant. For Austria, the total number of large-scale heatwaves is too small to obtain a meaningful result.

In summary, double jet stream events have an important influence on heatwaves in the northern area of Europe. This is most pronounced in the subregion Northern Europe. For the frequency of double jets no trends were found. Also a spatial change over time could not be observed. However, double jet configurations were found to be of regular occurrence; such a configuration could be detected on almost one third of the days in MJJASO in the studied period from 1979 to 2022.

In order to gain a better understanding of the double jet stream in the Northern Hemisphere and its effect on other weather extremes, the scope of future analyses could be extended spatially beyond the European domain and temporally over the whole year.

Appendix

Appendix A.

Latitude and Altitude of the Double Jet Stream over Time

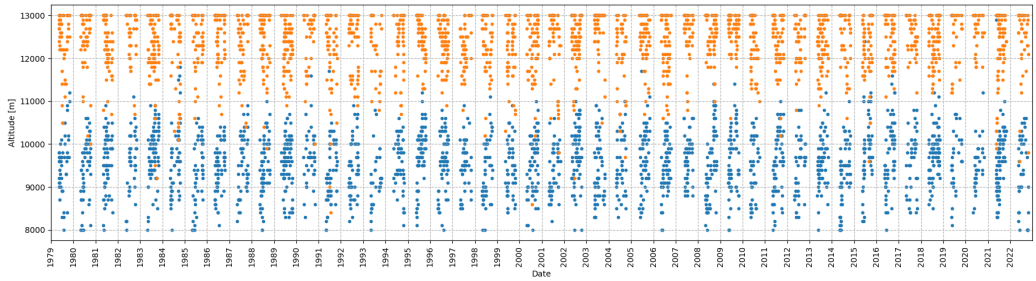


Figure A.1.: Altitudes in meter of detected double jets over time. For each double jet two points are marked, an orange and a blue one. They correspond to the two peaks that were found for each double jet. The higher altitude (orange) corresponds to the subtropical jet stream and the lower altitude (blue) to the polar jet stream.

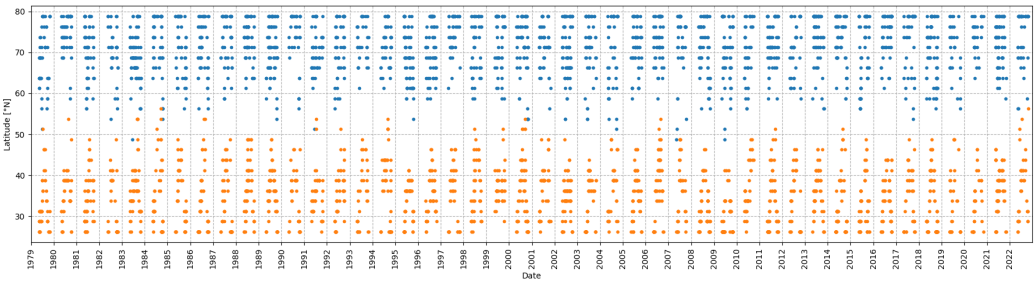


Figure A.2.: Latitudes in °N of detected double jets over time. For each double jet two points are marked, an orange and a blue one. They correspond to the two peaks that were found for each double jet. The higher latitude corresponds (blue) to the polar jet stream and the lower altitude (orange) to the subtropical jet stream.

Appendix B.

Double Jet Events with a certain Event Duration over Time



Figure B.1.: Number of Double Jet Events with a certain minimal duration over time (MJJASO from 1979 to 2022) with a linear fit (red line). Panels **a-l** show the frequency for a minimal duration of 1-12 days, respectively. No statistically significant trend could be detected, regardless of the minimum duration chosen. For longer events the number was too low for a linear regression analysis, but also with visual evaluation no trend in the frequency over time could be detected.

List of Figures

2.1. The three large circulation cells and their approximate position above Earth . . . 4
2.2. Vertical view of the idealized atmospheric circulation . . . 5
2.3. The subpolar jet stream over Europe and the Atlantic in the characteristic meandering pattern . . . 6
2.4. The jet stream over Europe and the influence on weather . . . 7
2.5. A double jet stream over Europe . . . 8

3.1. Spatial area for the detection of double jet stream states . . . 17
3.2. Grid points for the analysis of Austrian heatwaves . . . 17
3.3. Regions for the analysis of European heatwaves . . . 17
3.4. Altitude-latitude planes for the double jet stream detection . 19
a. Example of an altitude-latitude plane for a single day with a double jet stream present . . . 19
b. Example of an altitude-latitude plane with no double jet stream present . . . 19

4.1. Double jet stream days per half-year (MJJASO) . . . 25
4.2. Double Jet Stream Frequency . . . 28
a. Per Year . . . 28
b. Per Month . . . 28
4.3. Duration of the longest double jet event per year with Levene's test. . . . 28
4.4. Monthly occurrence of the longest double jet event of each half-year . . . 28
4.5. Moving variance of the duration of the longest double jet event per year . . . 29
4.6. Heatwave days per half-year (MJJASO) in Europe . . . 33
a. Yearly counts . . . 33
b. Grid point counts . . . 33
4.7. Heatwave days per half-year (MJJASO) in Western Europe . . 33
a. Yearly counts . . . 33
b. Grid point counts . . . 33
4.8. Heatwave days per half-year (MJJASO) in Eastern Europe . . 34
a. Yearly counts . . . 34
b. Grid point counts . . . 34

4.9. Heatwave days per half-year (MJJASO) in Northern Europe . 34
a. Yearly counts 34
b. Grid point counts 34
4.10. Heatwave days per half-year (MJJASO) in Austria 35
a. Yearly counts 35
b. Grid point counts 35
4.11. Heatwave days per half-year (MJJASO) in Austria with the spatial extent condition 35
a. Yearly counts 35
b. Grid point counts 35
4.12. Distribution of the random heatwave frequencies 39
a. Western Europe 39
b. Eastern Europe 39
c. Northern Europe 39
d. Austria 39
e. Austria (with spatial condition) 39
4.13. Joint appearance of heatwaves and double jets in Western Europe 41
a. Yearly count of days with a double jet event and a heatwave 41
b. Separate double jet and heatwave days per year 41
4.14. Correlation between detrended double jet days and heatwave days per half-year in Western Europe 41
4.15. Correlation between detrended double jet days and heatwave days per half-year in Eastern Europe 42
4.16. Correlation between detrended double jet days and heatwave days per half-year in Northern Europe 42
4.17. Correlation between detrended double jet and heatwave days per half-year in Austria 42
a. Austria 42
b. Austria (with spatial condition) 42
4.18. European heatwaves coinciding with double jet events 43
a. Heatwave count 43
b. Heatwave percentage 43
4.19. Double jet persistence and heatwave cumulative intensity - Western Europe 46
a. Scatter plot 46
b. Grid point counts 46
4.20. Double jet persistence and heatwave cumulative intensity - Eastern Europe 46
a. Scatter plot 46
b. Grid point counts 46

4.21. Double jet persistence and heatwave cumulative intensity - Northern Europe 47
a. Scatter plot 47
b. Grid point counts 47
4.22. Double jet persistence and heatwave cumulative intensity - Austria (with spatial condition) 48
a. Scatter plot 48
b. Grid point counts 48
4.23. Double jet persistence and heatwave cumulative intensity - Austria 48
a. Scatter plot 48
b. Grid point counts 48
4.24. Monthly occurrence of heatwaves that can be attributed to a double jet stream event 50
a. Western Europe 50
b. Eastern Europe 50
c. Northern Europe 50
d. Austria (with spatial condition) 50
e. Europe 50

A.1. Altitudes of detected double jets over time 61
A.2. Latitudes of detected double jets over time 61

B.1. Number of Double Jet Events with a certain minimal duration over time 64

List of Tables

4.1. Results of the Monte-Carlo analysis 38

Bibliography

Alizadeh, O., & Lin, Z. (2021). Rapid Arctic warming and its link to the waviness and strength of the westerly jet stream over West Asia. *Global and Planetary Change*, *199*, 103447. https://doi.org/10.1016/j.gloplacha.2021.103447 (cit. on pp. 10, 11)

Baede, A., Ahlonsou, E., Ding, Y., & Schimel, D. (2001). The climate system: An overview. In *Tar climate change 2001: The scientific basis*. IPCC. (Cit. on p. 3).

Barnes, E. A., & Screen, J. A. (2015). The impact of Arctic warming on the midlatitude jet-stream: Can it? Has it? Will it? *WIREs Climate Change*, *6*(3), 277–286. https://doi.org/10.1002/wcc.337 (cit. on pp. 9, 12)

Beccario, C. (2023). About earth :: A global map of wind, weather, and ocean conditions. Retrieved December 14, 2023, from https://earth.nullschool.net.html. (Cit. on p. 8)

Bednar-Friedl, B., Biesbroek, R., Schmidt, D., Alexander, P., Børsheim, K., J., C., Georgopoulou, E., Haasnoot, M., G. Le Cozannet, G., Lionello, P., Lipka, O., Möllmann, C., Muccione, V., Mustonen, T., Piepenburg, D., Whitmarsh, L., & (IPCC), I. P. O. C. C. (2022). Europe. In *Climate Change 2022 – Impacts, Adaptation and Vulnerability: Working Group II Contribution to the Sixth Assessment Report of the Intergovernmental Panel on Climate Change* (1st ed.). Cambridge University Press. https://doi.org/10.1017/9781009325844. (Cit. on pp. 1, 12, 31)

Belmecheri, S., Babst, F., Hudson, A. R., Betancourt, J., & Trouet, V. (2017). Northern Hemisphere Jet Stream Position Indices as Diagnostic Tools for Climate and Ecosystem Dynamics. *Earth Interactions*, *21*(8), 1–23. https://doi.org/10.1175/EI-D-16-0023.1 (cit. on p. 12)

Brunner, L., Hegerl, G. C., & Steiner, A. K. (2017). Connecting Atmospheric Blocking to European Temperature Extremes in Spring. *Journal of Climate*, *30*(2), 585–594. https://doi.org/10.1175/JCLI-D-16-0518.1 (cit. on pp. 1, 20)

Cohen, J., Zhang, X., Francis, J., Jung, T., Kwok, R., Overland, J., Ballinger, T. J., Bhatt, U. S., Chen, H. W., Coumou, D., Feldstein, S., Gu, H., Handorf, D., Henderson, G., Ionita, M., Kretschmer, M., Laliberte, F., Lee, S., Linderholm, H. W., ... Yoon, J. (2020). Divergent consensuses on Arctic amplification influence on midlatitude severe winter weather. *Nature Climate Change*, *10*(1), 20–29. https://doi.org/10.1038/s41558-019-0662-y (cit. on pp. 9, 11)

Connolly, C., Barnes, E. A., Hassanzadeh, P., & Pritchard, M. (2023). Using Neural Networks to Learn the Jet Stream Forced Response from Natural Variability [arXiv:2301.00496 [physics]]. Retrieved July 11, 2023, from http://arxiv.org/abs/2301.00496. (Cit. on p. 11)

Coumou, D., Kornhuber, K., Lehmann, J., & Petoukhov, V. (2017). Weakened Flow, Persistent Circulation, and Prolonged Weather Extremes in Boreal Summer. In S.-Y. S. Wang, J.-H. Yoon, C. C. Funk, & R. R. Gillies (Eds.), *Geophysical Monograph Series* (pp. 61–73). John Wiley & Sons, Inc. https://doi.org/10.1002/9781119068020.ch4. (Cit. on pp. 9–12)

Coumou, D., Petoukhov, V., Rahmstorf, S., Petri, S., & Schellnhuber, H. J. (2014). Quasi-resonant circulation regimes and hemispheric synchronization of extreme weather in boreal summer. *Proceedings of the National Academy of Sciences*, *111*(34), 12331–12336. https://doi.org/10.1073/pnas.1412797111 (cit. on pp. 7, 8, 12)

Deng, K.-Q., Azorin-Molina, C., Yang, S., Hu, C.-D., Zhang, G.-F., Minola, L., Vicente-Serrano, S., & Chen, D. (2022). Shifting of summertime weather extremes in Western Europe during 2012–2020. *Advances in Climate Change Research*, *13*(2), 218–227. https://doi.org/10.1016/j.accre.2022.01.008 (cit. on pp. 11, 12)

Fischer, E. M., & Schär, C. (2010). Consistent geographical patterns of changes in high-impact European heatwaves. *Nature Geoscience*, *3*(6), 398–403. https://doi.org/10.1038/ngeo866 (cit. on p. 19)

Fragkoulidis, G. (2022). Decadal variability and trends in extratropical Rossby wave packet amplitude, phase, and phase speed [Publisher: Copernicus GmbH]. *Weather and Climate Dynamics*, *3*(4), 1381–1398. https://doi.org/10.5194/wcd-3-1381-2022 (cit. on pp. 11, 52)

Francis, J., & Skific, N. (2015). Evidence linking rapid Arctic warming to mid-latitude weather patterns. *Philosophical transactions. Series A, Mathematical, physical, and engineering sciences*, *373*. https://doi.org/10.1098/rsta.2014.0170 (cit. on p. 9)

Galfi, V. M., & Messori, G. (2023). Persistent anomalies of the North Atlantic jet stream and associated surface extremes over Europe. *Environmental Research Letters*, *18*(2), 024017. https://doi.org/10.1088/1748-9326/acaedf (cit. on p. 12)

Garrett, J. (2013). A Rough Guide to the Jet Stream: What it is, how it works and how it is responding to enhanced Arctic warming. Retrieved December 14, 2023, from https://skepticalscience.com/jetstream-guide.html. (Cit. on p. 7)

Goosse, H. (2015). *Climate System Dynamics and Modelling:* (1st ed.). Cambridge University Press. https://doi.org/10.1017/CBO9781316018682. (Cit. on pp. 5, 6, 10)

Hallam, S., Josey, S. A., McCarthy, G. D., & Hirschi, J. J.-M. (2022). A regional (land–ocean) comparison of the seasonal to decadal variability of the Northern Hemisphere jet stream 1871–2011. *Climate Dynamics*, *59*(7-8), 1897–1918. https://doi.org/10.1007/s00382-022-06185-5 (cit. on p. 11)

Haslwanter, T. (2016). *An introduction to statistics with python*. Springer. https://doi.org/https://doi.org/10.1007/978-3-030-97371-1. (Cit. on pp. 20, 21, 52)

Hersbach, H., Bell, B., Berrisford, P., Hirahara, S., Horányi, A., Muñoz-Sabater, J., Nicolas, J., Peubey, C., Radu, R., Schepers, D., Simmons, A., Soci, C., Abdalla, S., Abellan, X., Balsamo, G., Bechtold, P., Biavati, G., Bidlot, J., Bonavita, M., ... Thépaut, J.-N. (2020). The ERA5 global reanalysis. *Quarterly Journal of the Royal Meteorological Society*, *146*(730), 1999–2049. https://doi.org/10.1002/qj.3803 (cit. on p. 15)

Jain, P., & Flannigan, M. (2021). The relationship between the polar jet stream and extreme wildfire events in North America. *Journal of Climate*, 1–59. https://doi.org/10.1175/JCLI-D-20-0863.1 (cit. on pp. 9, 12)

Kornhuber, K., Coumou, D., Vogel, E., Lesk, C., Donges, J. F., Lehmann, J., & Horton, R. M. (2020). Amplified Rossby waves enhance risk of concurrent heatwaves in major breadbasket regions. *Nature Climate Change*, *10*(1), 48–53. https://doi.org/10.1038/s41558-019-0637-z (cit. on pp. 1, 12)

Lee, S. H., Williams, P. D., & Frame, T. H. A. (2019). Increased shear in the North Atlantic upper-level jet stream over the past four decades. *Nature*, *572*(7771), 639–642. https://doi.org/10.1038/s41586-019-1465-z (cit. on p. 12)

Leyva, S. (2018). Atmospheric Circulation. Retrieved August 14, 2023, from http://geophile.net/Lessons/atmosphere/atm_circulation_04.html. (Cit. on p. 4)

Lupo, A. R. (2021). Atmospheric blocking events: A review. *Annals of the New York Academy of Sciences*, *1504*(1), 5–24. https://doi.org/10.1111/nyas.14557 (cit. on p. 8)

Maher, P., Kelleher, M. E., Sansom, P. G., & Methven, J. (2020). Is the subtropical jet shifting poleward? *Climate Dynamics*, *54*(3-4), 1741–1759. https://doi.org/10.1007/s00382-019-05084-6 (cit. on p. 11)

Mann, M. E., Rahmstorf, S., Kornhuber, K., Steinman, B. A., Miller, S. K., & Coumou, D. (2017). Influence of Anthropogenic Climate Change on Planetary Wave Resonance and Extreme Weather Events. *Scientific Reports*, *7*(1), 45242. https://doi.org/10.1038/srep45242 (cit. on p. 1)

Messori, G., Wu, M., Vico, G., & Galfi, V. M. (2022). Atmospheric jet stream variability reflects vegetation activity in Europe. *Agricultural and Forest Meteorology*, *322*, 109008. https://doi.org/10.1016/j.agrformet.2022.109008 (cit. on p. 1)

MetOffice. (2018). Global circulation patterns. Retrieved August 14, 2023, from https://www.metoffice.gov.uk/weather/learn-about/weather/atmosphere/global-circulation-patterns. (Cit. on p. 3)

Moon, W., Kim, B.-M., Yang, G.-H., & Wettlaufer, J. S. (2022). Wavier jet streams driven by zonally asymmetric surface thermal forcing. *Proceedings of the National Academy of Sciences*, *119*(38), e2200890119. https://doi.org/10.1073/pnas.2200890119 (cit. on pp. 10, 11)

NASA/Goddard Space Flight Center Scientific Visualization Studio. (2011). The polar jet stream. Retrieved December 14, 2023, from https://svs.gsfc.nasa.gov/3864. (Cit. on p. 6)

Nugent, A., & DeCou, D. (2019). Chapter 11: General Circulation [Book Title: Atmospheric Processes and Phenomena]. In *Atmospheric Processes and Phenomena*. University of Hawai'i at Manoa. Retrieved August 14, 2023, from http://pressbooks-dev.oer.hawaii.edu/atmo/chapter/chapter-11-general-circulation/. (Cit. on p. 6)

Pena-Ortiz, C., Gallego, D., Ribera, P., Ordonez, P., & Alvarez-Castro, M. D. C. (2013). Observed trends in the global jet stream characteristics during the second half of the 20th century: TRENDS IN THE GLOBAL JET STREAMS. *Journal of Geophysical Research: Atmospheres*, *118*(7), 2702–2713. https://doi.org/10.1002/jgrd.50305 (cit. on p. 11)

Perkins, S. E. (2015). A review on the scientific understanding of heatwaves—Their measurement, driving mechanisms, and changes at the global scale. *Atmospheric Research*, *164-165*, 242–267. https://doi.org/10.1016/j.atmosres.2015.05.014 (cit. on p. 1)

Perlwitz, J., Knutson, T., Kossin, J. P., & LeGrande, A. N. (2017). *Large-scale circulation and climate variability. In: Climate Science Special Report: Fourth National Climate Assessment, Volume I Climate Science Special Report* (tech. rep.). U.S. Global Change Research Program, Washington, DC. Retrieved July 14, 2023, from https://science2017.globalchange.gov/chapter/5/. (Cit. on p. 5)

Perlwitz, J. (2011). Tug of war on the jet stream [Number: 1 Publisher: Nature Publishing Group]. *Nature Climate Change*, *1*(1), 29–31. https://doi.org/10.1038/nclimate1065 (cit. on p. 9)

Rikus, L. (2018). A simple climatology of westerly jet streams in global reanalysis datasets part 1: Mid-latitude upper tropospheric jets. *Climate Dynamics*, *50*(7-8), 2285–2310. https://doi.org/10.1007/s00382-015-2560-y (cit. on p. 18)

Rodriguez Solis, J. L., Turrent, C., & Gross, M. (2022). Regional Responses of the Northern Hemisphere Subtropical Jet Stream to Reduced Arctic Sea Ice Extent. *Climate*, *10*(7), 108. https://doi.org/10.3390/cli10070108 (cit. on p. 11)

Rousi, E., Fink, A. H., Andersen, L. S., Becker, F. N., Beobide-Arsuaga, G., Breil, M., Cozzi, G., Heinke, J., Jach, L., Niermann, D., Petrovic, D.,

Richling, A., Riebold, J., Steidl, S., Suarez-Gutierrez, L., Tradowsky, J., Coumou, D., Düsterhus, A., Ellsäßer, F., ... Xoplaki, E. (2022b). The extremely hot and dry 2018 summer in central and northern Europe from a multi-faceted weather and climate perspective. https://doi.org/10.5194/egusphere-2022-813 (cit. on p. 12)

Rousi, E., Kornhuber, K., Beobide-Arsuaga, G., Luo, F., & Coumou, D. (2022a). Accelerated western European heatwave trends linked to more-persistent double jets over Eurasia. *Nature Communications*, *13*(1), 3851. https://doi.org/10.1038/s41467-022-31432-y (cit. on pp. 1, 9, 11, 12, 16, 18, 19, 22, 26, 27, 51)

Russo, S., Sillmann, J., & Fischer, E. M. (2015). Top ten European heatwaves since 1950 and their occurrence in the coming decades. *Environmental Research Letters*, *10*(12), 124003. https://doi.org/10.1088/1748-9326/10/12/124003 (cit. on p. 19)

Seneviratne, S. I., Zhang, X., Adnan, M., Badi, W., Dereczynski, C., Di Luca, A., Ghosh, S., Iskander, I., Kossin, J., Lewis, S., Otto, F., Pinto, I., Satoh, M., Vicente-Serrano, S. M., Wehner, M., & Zhou, B. (2021). Weather and Climate Extreme Events in a Changing Climate (Chapter 11). In V. Masson-Delmotte, P. Zhai, A. Pirani, S. L. Connors, C. Péan, S. Berger, N. Caud, Y. Chen, L. Goldfarb, M. I. Gomis, M. Huang, K. Leitzell, E. Lonnoy, J. B. R. Matthews, T. K. Maycock, T. Waterfield, K. Yelekçi, R. Yu, & B. Zhu (Eds.). Cambridge University Press. Retrieved November 21, 2023, from https://www.ipcc.ch/report/ar6/wg1/. (Cit. on p. 1)

Stendel, M., Francis, J., White, R., Williams, P. D., & Woollings, T. (2021). The jet stream and climate change. In *Climate Change* (pp. 327–357). Elsevier. https://doi.org/10.1016/B978-0-12-821575-3.00015-3. (Cit. on pp. 1, 3, 5, 6, 8, 10–12)

Taylor, P. C., Boeke, R. C., Boisvert, L. N., Feldl, N., Henry, M., Huang, Y., Langen, P. L., Liu, W., Pithan, F., Sejas, S. A., & Tan, I. (2022). Process Drivers, Inter-Model Spread, and the Path Forward: A Review of Amplified Arctic Warming. *Frontiers in Earth Science*, *9*. Retrieved September 18, 2023, from https://www.frontiersin.org/articles/10.3389/feart.2021.758361 (cit. on p. 10)

Trouet, V., Babst, F., & Meko, M. (2018). Recent enhanced high-summer North Atlantic Jet variability emerges from three-century context. *Nature Communications*, *9*(1), 180. https://doi.org/10.1038/s41467-017-02699-3 (cit. on p. 11)

Woollings, T. (2019). *Jet Stream: A Journey Through Our Changing Climate*. Oxford University Press. Retrieved August 19, 2023, from https://global.oup.com/academic/product/jet-stream-9780192845313?cc=at&lang=en&#. (Cit. on pp. 1, 6)

Woollings, T., Drouard, M., O'Reilly, C. H., Sexton, D. M. H., & McSweeney, C. (2023). Trends in the atmospheric jet streams are emerging in observations and could be linked to tropical warming. *Communications Earth & Environment*, *4*(1), 125. https://doi.org/10.1038/s43247-023-00792-8 (cit. on pp. 11, 52)

Wu, Q., Kang, C., Chen, Y., & Yao, Y. (2023). Significant weakening effects of Arctic sea ice loss on the summer western hemisphere polar jet stream and troposphere vertical wind shear. *Climate Dynamics*. https://doi.org/10.1007/s00382-023-06812-9 (cit. on pp. 10–12)

Xu, G., Broadman, E., Meko, M., Klippel, L., Ludlow, F., Dorado-Liñan, I., Esper, J., & Trouet, V. (2022). *800 years of summer European-North Atlantic jet stream variability and its impact on climate extremes and human systems* (other). display. https://doi.org/10.5194/egusphere-egu22-3331. (Cit. on p. 7)

Double jet stream states are a special configuration of the jet stream in which the jet stream splits into two distinct branches. Persistent weather conditions can prevail in the centre, which is particularly important for prolonged weather extremes. This thesis investigates trends in the occurrence and frequency of double jet stream configurations and their relationship to heatwaves in Europe with a special focus on Austria. Two algorithms are developed for the detection of double jets and heatwaves. They are applied to ERA5 reanalysis data for the extended summer period (May to October) from 1979 to 2022. The results show that, on average, a double jet event was present over the European area on 30 percent of all days in the period studied. No significant increase or decrease was found for the frequency of double jet events over time. The number of heatwave days in Europe, however, has doubled since 1979, and even a tripled for the Western and Eastern European subregions. Findings show that a double jet event is particularly relevant for heatwave occurrences in Europe north of 50°N. Here, 30 percent to a maximum of 60 percent of all heatwaves can be attributed to a double jet event. A significant link between double jets and heatwaves can be established for the subregions of Western Europe, Eastern Europe, and Northern Europe. The strongest influence is found in Northern Europe, where a statistically significant correlation between heatwave days and double jet days per year was established (correlation coefficient = 0.47, p-value = 0.01). Furthermore, longer double jet events can be connected with more intense heatwaves in Northern Europe. For the region of Austria, no statistically significant connection between double jets and heatwaves was detected. The results obtained in this thesis help to understand the characteristics and the effects of double jet stream states in recent years. They show that double jets have an important influence on the occurrence of heatwaves, especially in the northern parts of Europe.

Doppeljetstreams sind eine besondere Konfiguration des Jetstream, bei der sich der Jet in zwei Zweige aufspaltet. In der Mitte können anhaltende Wetterbedingungen herrschen, was besonders wichtig für lang anhaltende Wetterextreme ist. In dieser Arbeit werden Trends im Auftreten und in der Häufigkeit von Doppeljetstream-Konfigurationen und ihre Beziehung zu Hitzewellen in Europa mit einem speziellen Fokus auf Österreich untersucht. Es werden zwei Algorithmen für die Detektion von Doppeljets und Hitzewellen entwickelt. Diese werden auf ERA5-Reanalysedaten für den erweiterten Sommer (Mai bis Oktober) von 1979 bis 2022 angewandt. Die Ergebnisse zeigen, dass im Durchschnitt an 30 Prozent aller Tage im untersuchten Zeitraum ein Doppeljet-Event über dem europäischen Gebiet auftrat. Es wurde keine signifikante Zunahme oder Abnahme der Häufigkeit von Doublejet-Events im Laufe der Zeit festgestellt. Die Zahl der Hitzewellentage in Europa hat sich jedoch seit 1979 verdoppelt und in West- und Osteuropa sogar verdreifacht. Die Ergebnisse zeigen, dass ein Doublejet-Event besonders relevant für Hitzewellen in Europa nördlich von 50°N ist. Hier können 30 Prozent bis maximal 60 Prozent aller Hitzewellen mit einem Doublejet-Event in Verbindung gebracht werden. Ein signifikanter Zusammenhang zwischen Doppeljets und Hitzewellen kann für die Teilregionen Westeuropa, Osteuropa und Nordeuropa festgestellt werden. Der stärkste Einfluss ist in Nordeuropa feststellbar, wo eine statistisch signifikante Korrelation zwischen Hitzewellentagen und Doppeljet-Tagen pro Jahr festgestellt wurde (Korrelationskoeffizient = 0.47, p-Wert = 0.01). Außerdem können längere Doppeljet-Events mit intensiveren Hitzewellen in Nordeuropa in Verbindung gebracht werden. Für die Region Österreich lässt sich kein statistisch signifikanter Zusammenhang zwischen Doppeljets und Hitzewellen feststellen. Die in dieser Arbeit gewonnenen Ergebnisse tragen dazu bei, die Charakteristika und die Auswirkungen von Doublejetstream-Konfigurationen in den letzten Jahren zu verstehen. Sie zeigen, dass Doppeljets einen wichtigen Einfluss auf das Auftreten von Hitzewellen haben, insbesondere in den nördlichen Teilen Europas.

SR 102 | 2024 Double jet stream states and impacts on European heatwaves with a special focus on Austria
Wegener Center Verlag, University of Graz, Austria. ISBN 978-3-9505053-1-3